Integrated analysis of microbiome and metabolome reveals disease-specific profiles in inflammatory bowel diseases and intestinal Behçet's disease

Yehyun Park

Department of Medicine

The Graduate School, Yonsei University

Integrated analysis of microbiome and metabolome reveals disease-specific profiles in inflammatory bowel diseases and intestinal Behçet's disease

Directed by Professor Jae Hee Cheon

The Doctoral Dissertation
submitted to the Department of Medicine,
the Graduate School of Yonsei University
in partial fulfillment of the requirements for the degree of
Doctor of Philosophy in Medicine

Yehyun Park

December 2023

This certifies that the Doctoral Dissertation of
Yehyun Park is approved.

Thesis Supervisor : Jae Hee Cheon

Thesis Committee Member#1 : Tae Il Kim

Thesis Committee Member#2 : Seung Won Kim

Thesis Committee Member#3: Je Wook Yu

Thesis Committee Member#4: Jong Pil Im

The Graduate School
Yonsei University

December 2023

ACKNOWLEDGEMENTS

First and foremost, I would like to express my heartfelt gratitude to Prof. Jae Hee Cheon, who is not only my academic advisor but also the guiding force that led me into the field of Gastroenterology. Prof. Cheon has consistently provided me with invaluable guidance and unwavering support, and continues to do so. It is thanks to him that I am where I am today, and his belief in me has empowered me to move forward.

I would also like to extend my gratitude to my committee members: Prof. Tae Il Kim, Prof. Seung Won Kim, Prof. Je Wook Yu, and Prof. Jong Pil Im. Their advice has been instrumental in overcoming the challenges of my doctoral journey, and their expertise has greatly enriched the quality of this work.

Furthermore, I want to thank Dr. Sooyun Chang, who shared the role of chief resident with me and offered tremendous emotional support, as well as my junior colleague, Jae Bum Ahn, who assisted with data organization.

I am also deeply thankful to my beloved daughter, Suhbeen Shin, and my husband, Sanghoon Shin, for their understanding and unwavering support amidst my busy life. To my precious parents, who have always believed in me and devoted their unconditional love and dedication, I offer my sincerest gratitude and love.

Yehyun Park

<TABLE OF CONTENTS>

LIST OF FIGURES

LIST OF TABLES

ABSTRACT

Integrated analysis of microbiome and metabolome reveals disease-specific profiles in inflammatory bowel diseases and intestinal Behçet's disease

Yehyun Park

Department of Medicine
The Graduate School, Yonsei University

(Directed by Professor Jae Hee Cheon)

Background and aims: Gut microbial and metabolite alterations have been linked to the pathogenesis of inflammatory bowel diseases (IBD), including ulcerative colitis (UC) and Crohn's disease (CD). However, investigations into microbial and metabolic characteristics in intestinal Behçet's disease (BD), a condition sharing many clinical similarites with UC and CD, are largely lacking. The current study aimed to evaluate alterations in the gut microbiome and plasma metabolites in patients with intestinal BD, as well as UC and CD, compared with those in healthy controls. We also sought to discover microbial and metabolomic biomarkers that can aid in differentiating UC, CD, and intestinal BD.

Methods: Patients with IBD and intestinal BD undergoing diagnostic endoscopies, as well as healthy volunteers with endoscopy but no signs of inflammation, were enrolled. We conducted 16S ribosomal RNA (rRNA) sequencing on colon tissue samples obtained during colonoscopy and compared the diversity of microbial communities, taxonomic composition, and functional profiling between the control group and the UC, CD, and intestinal BD groups. Additionally, we collected and analyzed stool samples from the control group and IBD patients for 16S rRNA sequencing. Blood samples were drawn from the control group, UC, CD, and intestinal BD patients, and plasma metabolomic analysis was performed using gas chromatography time-of-flight mass spectrometry (GC–TOF–MS) and ultra-performance liquid chromatography–quadrupole/time-of-flight mass spectrometry (UPLC–Q–TOF–MS) analysis.

Results: A total of 100 patients (35 UC, 30 CD, and 35 BD) and 41 healthy volunteers were enrolled in the study. We conducted 16S rRNA sequencing on 73 tissue samples (12 control, 24 UC, 14 CD, and 23 BD) and 19 stool samples (5 control, 9 UC, and 5 CD). Metabolite analysis was performed on 100 blood samples (25 control, 24 UC, 26 CD, and 25 BD). The microbial diversity of colon tissue was reduced only in CD, with no significant decrease observed in BD. The microbial taxonomic profile of intestinal BD displayed a pattern more similar to healthy controls than UC or CD, and it exhibited distinctive features setting it apart from both UC and CD. However, there were common changes across all three conditions (UC, CD, and BD), which is a decrease in five beneficial bacteria responsible for producing short-chain fatty acids: *Fusicatenibacter saccharivorans*, *Coprococcus comes*, *Blautia obeum*, *Dorea formicigenerans*, and *Roseburai ceciola*. Additional changes in intestinal BD included a decreased abundance of *Subdoligranulum variable* and *Blautia wexlerae*, which were shared features with either UC or CD. As a specific alteration unique to BD, a decrease in the genus *Bacteroides*, particularly the species *Bacteroides fragilis*, was identified. The metabolomic profile of intestinal BD was most similar to CD and distinct from both controls and UC. However, UC, CD, and BD each exhibited distinct metabolomic profiles. Overall, BD exhibited pronounced functional changes and metabolite alterations, including changes in energy metabolism, amino acid, carbohydrate, and lipid metabolism, cofactor and vitamin metabolism, nucleotide metabolism, and genetic information processing, while not showing as substantial microbial taxonomic changes as UC or CD. The microbial functions analyzed by phylogenetic investigation of communities by reconstruction of unobserved states (PICRUSt) showed a good alignment with the enriched pathways identified by qualitative enrichment analysis of plasma metabolite.

Conclusion: In this integrative analysis of microbiome and metabolome in IBD and intestinal BD, we observed that intestinal BD exhibited profiles that were both shared with and distinct from those of the control group, UC, and CD.

Key words : intestinal Behçet’s disease, ulcerative colitis, Crohn’s disease, microbiome, metabolome, multi-omics

Integrated analysis of microbiome and metabolome reveals disease-specific profiles in inflammatory bowel diseases and intestinal Behçet's disease

Yehyun Park

Department of Medicine
The Graduate School, Yonsei University

(Directed by Professor Jae Hee Cheon)

I. INTRODUCTION

Crohn's disease (CD) and ulcerative colitis (UC) are inflammatory bowel disease (IBD), a chronic inflammatory disorder of the gastrointestinal tract that is related to dysbiosis and altered interactions between the dysbiotic microbiota and host intestinal immune system.[1] In CD, transmural inflammation can occur throughout the entire gastrointestinal tract, whereas in UC, inflammation is confined to the mucosal layer of the colon. Behçet's disease (BD) is a chronic relapsing systemic inflammatory disorder of unknown origin characterized by oral and genital mucosal ulcers, uveitis, skin lesions, and neurological, or gastrointestinal manifestations. The prevalence of intestinal involvement in patients with BD has been reported in the range of 2.8% to 50% with a remarkable geographic variation, which is more frequent in East Asia, including Korea and Japan, than in other areas of the world.[2] There exist many similarities between IBD and intestinal BD. Both have chronic inflammation in the gastrointestinal tract, similar extraintestinal manifestations, and chronic fluctuating courses characterized by repeated episodes of relapse and remission. IBD and intestinal BD may be closely related and be a part of a spectrum of diseases, rather than distinct disease entities. Regarding the pathogenesis of BD, it is postulated that similar to IBD, the involvement of triggering factors such as infection occurs in genetically predisposed patients.[3] However, due to its rarity in Western countries, the understanding of BD remains significantly less established compared to IBD. While numerous studies have suggested the involvement of intestinal

microbiota in the pathogenesis of IBD, such investigations are largely lacking in the context of intestinal BD.

Metagenomics is defined as the analysis of the collective genomes that are present in a defined environment or ecosystem, hence giving insight into the functions of non-cultivated bacteria. The development of cultivation-independent methods based on next-generation sequencing rapidly expanded our knowledge about the fundamental role of the intestinal microbiome in the pathogenesis of microbiota in the gastrointestinal tract. Pyrosequencing can sequence 500 million bases, at 99% or better accuracy, in a single run. It represents an approximately 2,000-fold increase in throughput over Sanger sequencing, and many more sequences can be read as shorter sequences.[4] Bacteria that are in low abundance can be detected using this method. Metagenomic approaches can demonstrate the microbial diversity of the gut microbiota, qualitative and quantitative information on bacterial species, and changes in the gut microbiota in relation to disease. Although metagenomic shotgun sequencing enables precise taxonomic classification to species and strain level and can directly infer the relative abundance of microbial functional genes, this method is relatively expensive, laborious, and has a complex sample preparation and analysis process. Instead, 16S ribosomal RNA (16S rRNA) gene sequence analysis, also called marker gene analysis or amplicon sequencing, has the advantage of quick, simple, and relatively inexpensive sample preparation and analysis. 16S rRNA sequencing uses primers that target a specific region of a 16S rRNA gene in order to determine the bacterial phylogenies of a sample. This region contains a highly variable region that can be used for detailed identification that is flanked by highly conserved regions that can serve as binding sites for PCR primers. This approach is suitable for samples contaminated by host DNA such as tissue, and 16S rRNA gene sequencing generally correlates well with genomic content.

Previous studies have evaluated the composition of gut microbiota in IBD patients and confirmed significant differences of gut microbiota from that of healthy individuals.[5-11] However, previous studies have demonstrated heterogenous results of changes in the

intestinal microbiota in IBD patients, and limited data are available regarding BD. Also, knowing only the variations in microbial community structure is no longer adequate for a thorough understanding of the disease. An emerging field of study involves the integration of various chemical and biological data types through multi-omics analysis, aiming to offer a comprehensive, functional, and mechanistic understanding of complex biological systems. One of the data types integrated with marker gene sequencing is metabolite data. Metabolomics is the study of the metabolome; the metabolome is the collective array of metabolites present in a biological sample. Metabolomic data provide important information regarding molecules such as short-chain fatty acids or bile acids that are produced or modified by the gut microbiota that affect mucosal protection and immune regulatory functions. Due to the inherent limitations of 16S rRNA gene sequencing in estimating microbial community function, the integration of metabolomics provides a more comprehensive understanding of both the composition and function of microbial communities. Several studies identified metabolite differences in the stool,[12,13] serum,[13-15] or mucosa of IBD patients compared with controls. While fecal metabolites may better reflect the direct metabolic output of the microbiota, blood metabolites offer insight into the subset of these compounds that enter circulation, potentially influencing host metabolism and health. The advent of untargeted metabolomics has enhanced our comprehension of the blood metabolome and facilitated the detection of distinctive molecules in circulation, produced by the gut microbiota, and potentially exerting biological effects in the host. However, such a multi-omics approach has mainly been conducted within the broader context of IBD, and research distinguishing features between UC and CD is lacking. Specifically, there is a dearth of studies that integrate the characteristics of BD, UC, and CD for analysis.

The current study aimed to evaluate gut microbiome change in patients with intestinal BD as well as UC and CD, and to identify alterations in plasma metabolites in IBD and BD patients compared with healthy control. Through this study, we seek to discover

microbial and metabolomic markers that can aid in the diagnosis and differential diagnosis of UC, CD, and intestinal BD.

II. MATERIALS AND METHODS

1. Study subjects

We included patients aged 18 years and older with UC, CD, and intestinal BD from the IBD Clinic of Yonsei University College of Medicine, Severance Hospital, Seoul, Korea between January 2014 and January 2019. Patients with evidence of active infection or sepsis at the time of enrollment or those who received antibiotics within the prior 3 months were excluded from the study. The diagnosis of UC, CD, and intestinal BD is based upon the internationally accepted diagnostic criteria.[16-18] The diagnosis involved evaluating various factors, including clinical presentation, endoscopic findings or surgical observations, radiology, histology, and/or serology. For intestinal BD, only patients who were finally classified as “definite” or “probable” types were included in this study.[18] The healthy volunteer group without current acute active illness, renal failure, diabetes, congestive heart failure, and cirrhosis were enrolled.

The Institutional Review Board of Severance Hospital, Yonsei University approved this study (IRB approval number: 4-2013-0805). All patients and controls provided written informed consent and all methods were performed in accordance with the relevant guidelines and regulations.

2. Clinical data collection

Demographic factors, disease duration, location, surgery, medical treatment, disease activities, C-reactive protein (CRP), and albumin levels were collected. Disease activities were evaluated using the partial Mayo (pMayo) score for UC, Crohn’s disease activity index (CDAI) for CD, and the activity index for intestinal Behçet’s disease (DAIBD) for BD.[19] Disease severity was classified based on clinical scores. Remission was defined as pMayo below 2, CDAI below 150, and DAIBD below 20. Mild disease was defined as

pMayo of 2-4, CDAI 150-219, and DAIBD 20-39; moderate disease as pMayo of 5-7, CDAI 220-450, and DAIBD 40-74; and severe disease as pMayo score of 8 or higher, CDAI 451 or higher, and DAIBD 75 or higher.

3. Collecting tissue, blood, and stool samples

Tissue samples were collected at the time of colonoscopy. Three mucosal biopsies were retrieved from the ileocecal area using biopsy forceps and immediately snap-frozen in liquid nitrogen. The tissue was stored at -80 ℃ until further analysis. If there was active inflammation in the ileocecal area, biopsies were performed from non-ulcerated mucosa whenever possible. Stool samples were collected either at the time of colonoscopy or at the time of visiting out-patient clinic. In the case of collecting at the time of colonoscopy, stool before administration of bowel preparation was collected. Stool samples of 50~100 mg were kept at 4°C for less than 24 hours and were stored at -80°C until DNA extraction. For patients who consented to blood collection, 10 mL of blood was collected into an EDTA tube following a 9-hour fasting period. The collected blood was then transferred to the laboratory immediately. The blood was centrifuged at 1,500 × *g* for 15 min and each 300 μL aliquot was stored at -80 ℃ until further analysis.

4. Microbiome analysis

A. DNA extraction

Fecal samples or mucosal biopsy samples were resuspended in 50 mM Tris buffer (pH 7.5) containing 1 mM EDTA, 0.2% β-mercaptoethanol (Sigma-Aldrich, Burlington, MA, USA) and 1000 U/ml of lyticase (Sigma-Aldrich, Burlington, MA, USA). The mix is incubated at 37°C for 30 min and genomic DNA is isolated by using FastDNA™ SPIN Kit for Soil (MP Biomedicals, Irvine, CA, USA) according to the manufacturer's instructions. The extracted DNA was stored at -80 ℃ until analysis.

B. PCR amplification and 16S rRNA amplicon sequencing

PCR amplification was performed using barcoded fusion primers targeting the V1 to V3 regions of the 16S rRNA gene and the extracted DNA as a template, using a C1000 Touch thermal cycler (Bio-Rad, Hercules, CA, U.S.A). The 16S universal primers 27F (5'-GAGTTTGATCMTGGCTCAG-3') and 518R (5'- WTTACCGCGGCTGCTGG-3') were used. For samples collected later, fusion primers 341F (5'- CCTACGGGNGGCWGCAG-3') and 805R (5'- GACTACHVGGGTATCTAATCC) targeting the V3 to V4 regions of the 16S rRNA gene were used. The PCR product was confirmed using 1% agarose gel electrophoresis and visualized under a Gel Doc system (BioRad, Hercules, CA, USA). Amplified products were purified using the QIAquick PCR purification kit (Qiagen, Valencia, CA, USA) and quantified using the PicoGreen dsDNA Assay kit (Invitrogen, Carlsbad, CA, USA). Equimolar concentrations of the purified amplicon from different samples were pooled and short fragments < 500 bp (non-target products) were removed using Ampure beads (Agencourt Bioscience, MA, USA). The quality and product size were assessed on a Bioanalyzer 2100 (Agilent, Palo Alto, CA, USA) using a DNA 7500 chip. Mixed amplicons were subjected to emulsion PCR and then sequenced. Pyrosequencing was carried out at ChunLab, Inc. (Seoul, Korea), using a GS FLX Titanium system (Roche, Branford, CT, USA) and Illumina MiSeq platform (Illumina, San Diego, California, USA).

C. Microbiome data analysis

Sequencing data were analyzed according to previous descriptions.[20-22] Reads obtained from the samples were categorized by means of the unique barcodes of each PCR product. The sequences of the barcode, linker, and primers were removed from the original sequencing reads. The quality of sequencing was checked manually by secondary-structure-aware alignment using the EzEditor program.[23] After eliminating non-specific amplicons, amplicons not assigned to the target taxon, and chimeras in the quality check process, the taxonomic classification of each read was analyzed using the EzBioCloud[24] using the database version PKSSU4.0, which is an up-to-date version for the prokaryotic

16S database. EzBioCloud contains 16S rRNA gene sequences of type strains that have valid published names and representative species-level phylotypes of either cultured or uncultured entries with complete hierarchical taxonomic classifications, from the phylum to the species levels. Calculations of alpha- and beta-diversity indices, biomarker discovery using linear discriminant analysis (LDA) effect size (LEfSe), and phylogenetic investigation of communities by reconstruction of unobserved states (PICRUSt) algorithms[25] were carried out after normalization based on 16S rRNA gene copy number variation. For alpha-diversity, we utilized the numbers of operational taxonomic units (OTUs) for richness, Simpson for evenness, and the Shannon index as a combined measure considering both richness and evenness. Beta-diversity was visualized by hierarchical cluster trees using the unweighted pair group method with arithmetic mean (UPGMA) and analyzed by Bray-Curtis and visualized using principal coordinate analysis (PCoA).[26,27] LEfSe was used to identify specific microbiota that were differentially distributed between different samples, which may be available as microbial biomarkers. The predictive functional profiling was described using the PICRUSt and annotated to their Kyoto Encyclopedia of Genes and Genomes (KEGG) pathways. Comparing taxonomic data and alpha-diversity between groups was performed using Mann-Whitney U test. Comparing beta-diversity between groups was performed using permutational multivariate analysis of variance (PERMANOVA), which is a non-parametric multivariate statistical test.[28] A p value of less than 0.05 was considered statistically significant.

5. Metabolomic analysis

A. Sample preparation for metabolomic analysis

Metabolites were extracted from 200 μL of plasma. One milliliter of methanol containing 10 μL of internal 2-chlorophenylalanine standard (1 mg/mL in water) was added to plasma samples and then homogenized using a mixer mill at a frequency of 30 Hz for 5 min and sonicator for 5 min. After homogenization, the suspension was held at 4 °C for 60 min, and then centrifuged at 20,000 × g and 4 °C for 10 min. The supernatant was filtered through a

0.2 μm polytetrafluoroethylene (PTFE) filter and evaporated using a speed vacuum concentrator (Modulspin 31, Biotron, Wonju, Korea). The final concentration of each analyzed sample was 10 mg/mL. Metabolomic analysis by mass spectrometry was carried out at MetaMass, Inc. (Seoul, Korea).

B. GC-TOF-MS analysis

Each sample of 100 μL was re-evaporated for derivatization. Dried samples were further oximated and silylated for gas chromatography time-of-flight mass spectrometry (GC–TOF–MS) analysis. For metabolite profiling, GC-TOF–MS analysis was performed using an Agilent 7890A gas chromatography system coupled with an Agilent 7693 autosampler (Agilent Technologies, Palo Alto, CA, USA) equipped with a Pegasus III TOF MS (LECO Corp., St. Joseph, MI, USA) system. An Rtx-5MS column (30 m × 0.25 mm, 0.25 μm particle size; Restek Corp., Bellefonte, PA, USA) was used with a constant flow of 1.5 mL/min of helium as the carrier gas. Derivatized samples of 1 μL were injected into the GC with splitless mode. The oven temperature was maintained at 75 °C for 2 min, then incrementally increased by 15 °C/min to 300 °C and held for 3 min as the final temperature. The temperatures of the front inlet and transfer line were 250 and 240 °C, respectively. The electron ionization was carried out at − 70 eV and full scanning over the range of 50–800 m/z was used for mass data collection.

C. UPLC-Q-TOF-MS analysis

Dried extracts were re-dissolved in 250 μL of methanol for ultra-performance liquid chromatography–quadrupole/time-of-flight mass spectrometry (UPLC–Q–TOF–MS) analysis. UPLC was performed on a Waters ACQUITY UPLC™ system (Waters Corp., Milford, MA, USA) equipped with a binary solvent delivery system, a UV detector, and an auto-sampler. Chromatographic separation was performed on a Waters ACQUITY UPLC BEH C18 column 100 mm × 2.1 mm, 1.7 μm particle size (Waters Corp., Milford, MA, USA), and the injection volume was 5 μL. The column temperature was set at 37 °C and

the flow rate was 0.3 mL/min. The mobile phase consisted of 0.1% v/v formic acid in water (Solvent A) and 0.1% v/v formic acid in acetonitrile (Solvent B). The total run time was 14 min, including re-equilibration of the column to the initial conditions. The gradient parameters were set as follows: 5% solvent B was maintained initially for 1 min, followed by a linear increase to 100% solvent B over 9 min, and then sustained at 100% solvent B for 1 min with a gradual decrease to 5% solvent B over 3 min. For MS experiments, the Waters Micromass Q–TOF Premier (Micromass MS Technologies, Manchester, UK) was operated in negative ion mode with an m/z range of 100–1000. The source temperature was set at 100 °C, the collision energy was set at 10 eV, the collision gas flow was 0.3 mL/min, and the desolvation gas was set to 650 L/h at a temperature of 300 °C. The capillary voltage and sample cone voltage were set at 2.5 kV and 50 V, respectively. The V mode was used for the mass spectrometer and data were collected in the centroid mode with a scan accumulation of 0.2 s. Leucine encephalin was used as reference lock mass (m/z 554.2615) by independent LockSpray interference.

D. Data analysis

The GC–TOF–MS data were acquired, pre-processed, and converted into the NetCDF format (*.cdf) using the LECO Chroma TOF™ software (version 4.44, LECO Corp., St. Joseph, MI, USA). The raw data from UPLC–Q–TOF–MS analysis were acquired and converted into the NetCDF format (*.cdf) using MassLynx software (version 4.1, Waters Corp., Milford, MA, USA) and MassLynx DataBridge software (version 4.1, Waters Corp., Milford, MA, USA). After conversion, peak detection, retention time correction, and alignment were processed using the MetAlign software (Wageningen Food Safety Research, Wageningen, Netherlands). The resulting alignment data were exported to a Microsoft Excel file.

Integrative metabolomic data analysis was performed using a web-based comprehensive metabolomics data processing tool, MetaboAnalyst 5.0 (http://www.metaboanalyst.ca). Each variable of the quantitative data was first normalized by the median value and then

log-transformed, centered and scaled to mean and standard deviation of each variable. Hierarchical cluster analysis was performed in order to identify clustering patterns and Spearman's rank correlation coefficient was used to evaluate the correlation between each pair of features. Dendrograms were visualized through heatmaps, where each colored cell on the map corresponds to a concentration value. To analyze differences between groups, analysis of variance (ANOVA) was performed on normalized data. To compare differential metabolites among control, UC, CD, and BD, and to explain the maximum separation among groups, unsupervised and supervised multivariate regression techniques, principal component analysis (PCA) and partial least squares discriminant analysis (PLS-DA), respectively, were performed. For each model, the optimal number of components was chosen according to the highest prediction accuracy (Q^2) estimated by the 5-fold cross-validation technique. The discriminative metabolites were selected based on variable importance in projection (VIP) values. VIP is one of the important measures of PLS-DA and is a weighted sum of squares of the PLS loadings taking into account the amount of explained class variation in each dimension. Metabolites were ranked according to their VIP scores and metabolites with VIP scores greater than 1 are considered as the significant contributors. To identify biologically meaningful patterns based on the metabolomics data, quantitative enrichment analysis [QEA] was carried out. Data were mapped to the KEGG human metabolic pathway database comprising 84 metabolite sets of normal metabolic pathways. QEA is based on the well-established globaltest[29] to test associations between metabolite sets and the outcome. The algorithm uses a generalized linear model to compute a 'Q-stat' for each metabolite set. The Q-stat is calculated as the average of the Q values calculated for each single metabolite, while the Q value is the squared covariance between the metabolite and the outcome. Spearman's rank correlation coefficient was used to analyze the correlation between microbiota and metabolites, and visualization was made in the form of a heat map.

6. Statistical analysis

Baseline characteristics were analyzed by descriptive statistics. For continuous variables, the median and range were reported. For comparing between two groups, Mann–Whitney *U* test was used. Comparing multiple groups was first analyzed by the Kruskal–Wallis *H* test and if $p < 0.05$, then pairwise comparisons using the Mann–Whitney *U* test were used to compare continuous variables. For categorical variables, frequency with percentage was reported and compared using Pearson's $\chi 2$ test or Fisher's exact test. Correlations were identified by Spearman's rank correlation coefficient. All results were considered statistically significant when the two-tailed *p* value was < 0.05. To control for false discovery rate (FDR), the resultant *p* values were then adjusted for multiple comparisons using the Benjamini and Hochberg method.[30] A FDR of 10%, or FDR-adjusted $p < 0.1$, was considered significant for microbial functional biomarker discovery and metabolites analysis.[14]

Statistical analysis and visualizing by chart were performed using SPSS version 20.0 (SPSS Inc., Chicago, IL, USA) and GraphPad Prism V.10.0 (GraphPad Software Inc., San Diego, CA, USA).

III. RESULTS

1. Study population

In total, 100 patients (35 UC, 30 CD, and 35 BD) and 41 healthy volunteers were eligible for enrollment. Each subject provided samples from one to three sources, including tissue, stool, and blood. Overall, 192 samples from 141 subjects were analyzed. We conducted 16S rRNA sequencing on 73 tissue samples (12 control, 24 UC, 14 CD, and 23 BD) and 19 stool samples (5 control, 9 UC, and 5 CD), and performed metabolite analysis on 100 blood samples (25 control, 24 UC, 26 CD, and 25 BD) (Figure 1). The sample status from 141 patients or controls is visualized in Figure 2. The clinical information of the patients and controls in each sample type is shown in Table 1.

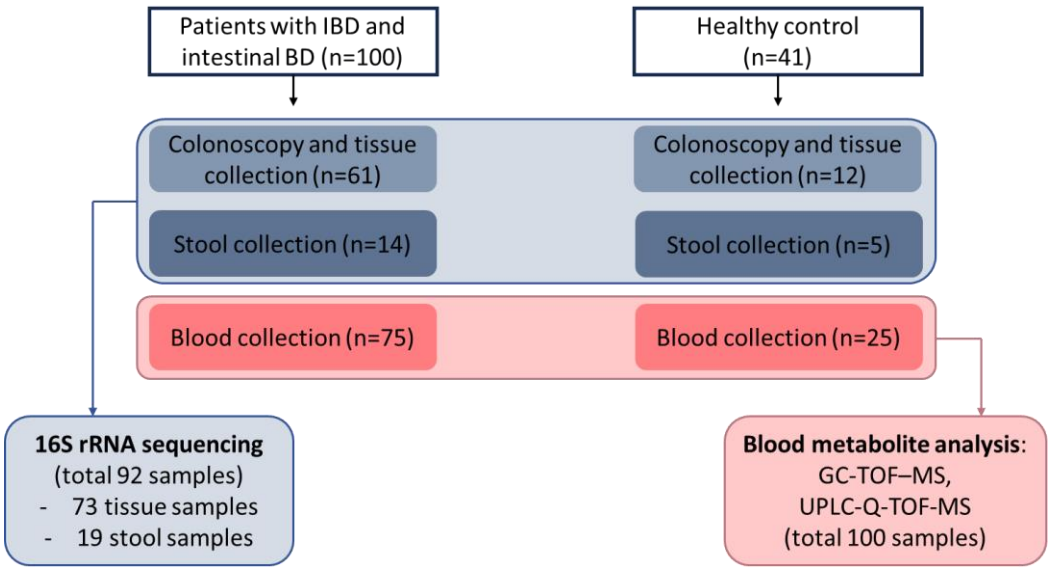

Figure 1. Flow diagram of the study. In total, 100 patients (35 UC, 30 CD, and 35 BD) and 41 healthy volunteers were eligible for enrollment. Each subject provided samples from one to three sources, including tissue, stool, and blood. Overall, 192 samples from 141 subjects were analyzed. IBD: inflammatory bowel disease, BD: Behçet's disease, rRNA: ribosomal ribonucleic acid, GC-TOF-MS: gas chromatography time-of-flight mass spectrometry, UPLC-Q-TOF-MS: ultra-performance liquid chromatography–quadrupole/time-of-flight mass spectrometry

Among the patients who underwent tissue microbiome analysis, the CD patient group exhibited a younger age, a higher prevalence of bowel resection history (21.4%), elevated CRP levels, and a higher frequency of immunomodulator usage (57.1%) compared to control, UC, and BD patients. In the case of BD, an increased use of steroids (43.5%) was observed. Based on the disease activity scores, clinical disease activity was divided into four categories (remission, mild, moderate, and severe). In UC, the proportion of mild cases was relatively high (41.7%), while in CD, remission was more prevalent (50.0%). In the case of BD, activity was distributed relatively evenly. Among the patients who underwent stool microbiome analysis, the CD patient group displayed a tendency towards a younger

age in comparison to controls or UC patients. Furthermore, CD patients demonstrated higher ESR levels and a greater frequency of immunomodulator (IMM) usage (80%). The clinical disease activity was distributed between remission to moderate activity. For patients who underwent plasma metabolite analysis, the CD patient group showed a younger age, a higher proportion of males (84.6 %), elevated CRP levels, and a greater frequency of IMM usage (57.7%). UC patients exhibited longer disease durations compared to CD or BD patients (32.1 months vs. 7.2 and 5.9 months). Additionally, in the context of BD, higher ESR levels and an elevated proportion of steroid usage were noted. Clinical disease activity showed that in UC, the proportion of mild cases was relatively high, while in CD, it ranged from remission to moderate. In the case of BD, activity was distributed relatively evenly. Among intestinal BD patients, 30% of tissue sample donors and 36% of blood sample donors had intestinal BD without systemic BD.

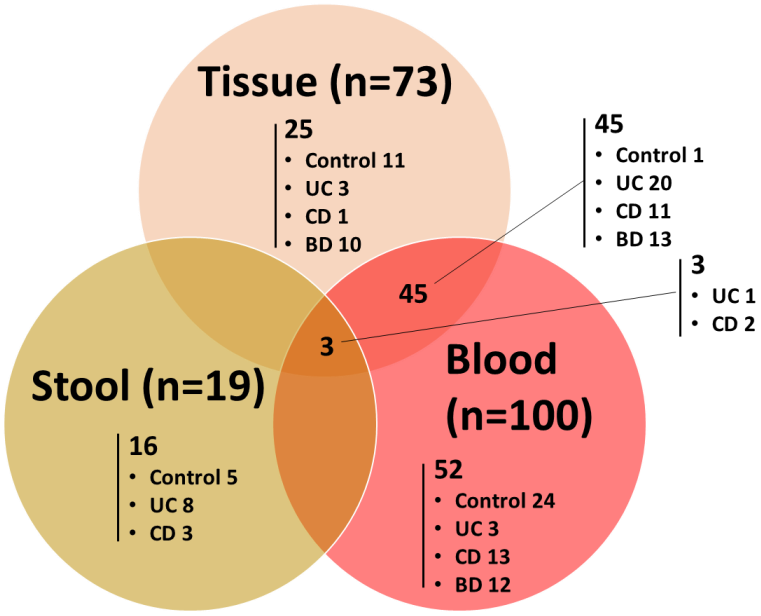

Figure 2. Venn diagram of collected samples of a total 141 patients or controls according to sample type. UC: ulcerative colitis, CD: Crohn's disease, BD: Behçet's disease

Table 1. Baseline clinical characteristics of enrolled patients and controls

	Tissue microbiome analysis (n=73)				*p*
Characteristics	Control (n=12)	UC (n=24)	CD (n=14)	BD (n=23)	
Age, median (range)	47.2 (32.1-74.2)	42.6 (19.5-68.6)	22.7 (18.0-31.5)	46.2 (25.8-76.5)	<0.001
Sex, male/female, n (%)	6 (50.0)/ 6 (50.0)	13 (54.2)/ 11 (45.8)	11 (78.6)/ 3 (21.4)	10 (43.5)/ 13 (56.5)	0.21
BMI, kg/m^2, median (range)	22.3 (15.6-26.8)	21.8 (16.1-28.7)	21.1 (13.9-22.9)	23.0 (16.0-28.0)	0.10
Bowel resection history, n (%)	0	0	3 (21.4)	1 (4.3)	0.03
Disease duration, months, median (range)	-	39.6 (24.0-65.6)	20.3 (7.5-28.3)	27.5 (6.8-72.7)	0.20†
Disease location, n (%)	-				
E1 (proctitis)	-	6 (25)	-	-	
E2 (left sided)	-	7 (29.2)	-	-	
E3 (pancolitis)	-	11 (45.8)	-	-	
L1 (ileal)	-	-	0	-	
L2 (colonic)	-	-	1 (7.1)	-	
L3 (ileocolic)	-	-	13 (92.9)	-	
With/without systemic BD, n (%)	-	-	-	16(69.6)/7(30.4)	
Disease activity, remission/mild/ moderate/severe, n (%)	-	2 (8.3)/10 (41.7)/7 (29.2)/5 (20.8)	7 (50.0)/2 (14.3)/5 (35.7)/0	4 (17.4)/6 (26.1)/7 (30.4)/6 (26.1)	0.05
Disease activity score, median (range)					
Partial Mayo score	-	4.5 (3.0-6.0)	-	-	
CDAI	-	-	148.5 (73.0-226.0)	-	
DAIBD	-	-	-	60.0 (22.5-70.0)	

Hb, g/dL, median (range)	13.0 (11.7-16.0)	13.5 (9.7-15.2)	12.9 (10.7-15.8)	13.1 (10.2-16.8)	0.63
ESR, mm/hr, median (range)	14.0 (2.0-62.0)	23.5 (2.0-52.0)	37.0 (3.0-99.0)	33.0 (8.0-106.0)	0.07
CRP, mg/L, median (range)	0.4 (0.3-0.5)	2.2 (0.8-3.9)	7.9 (2.3-23.6)	5.6 (1.5-13.9)	0.02
Albumin, g/dL, median (range)	4.3 (4.2-4.5)	4.2 (4.0-4.5)	4.0 (3.7-4.5)	4.4 (4.2-4.5)	0.14
Creatinine, mg/dL, median (range)	0.8 (0.5-1.0)	0.7 (0.5-1.1)	0.8 (0.5-1.0)	0.7 (0.5-1.4)	0.62
ALT, U/L, median (range)	18 (8.0-30.0)	9 (5.0-34.0)	9.5 (6.0-40.0)	20.0 (7.0-40.0)	<0.01
Medication, n (%)					
5-ASA	-	24 (100)	12 (85.7)	23 (100)	0.05†
Steroid	-	3 (12.5)	1 (7.1)	10 (43.5)	0.01†
IMM	-	5 (20.8)	8 (57.1)	5 (21.7)	0.04†
Anti-TNF	-	4 (16.7)	1 (7.1)	0	0.10†

	Stool microbiome analysis (n=19)			*p*
Characteristics	Control (n=5)	UC (n=9)	CD (n=5)	
Age, median (range)	22.0 (20.5-31.2)	44.3 (18.4-56.3)	18.0 (18.0-38.2)	0.05
Sex, male/female, n (%)	3 (60.0)/2 (40.0)	5 (55.6)/4 (44.4)	5 (100)/0	0.21
BMI, kg/m^2, median (range)	19.1 (18.9-22.8)	20.7 (16.8-23.3)	20.5 (16.3-29.6)	0.87
Bowel resection history, n (%)	0	1 (11.1)	1 (20.0)	1.00
Disease duration, months, median (range)	-	2.6 (1.0-46.0)	2.9 (2.0-12.0)	0.95†
Disease location, n (%)				
E1 (proctitis)	-	3 (33.3)	-	
E2 (left sided)	-	4 (44.4)	-	
E3 (pancolitis)	-	2 (22.2)	-	
L1 (ileal)	-	-	1 (20)	
L2 (colonic)	-	-	0	
L3 (ileocolic)	-	-	4 (80)	
With/without systemic BD, n (%)	-	-	-	
Disease activity, remission/mild/moderate/sev	-	4 (44.4)/4 (44.4)/1	1 (20.0)/2 (40.0)/2	0.63

ere, n (%)		(33.3)/0	(40.0)/0	
Disease activity score, median (range)				
Partial Mayo score	-	2.0 (1.0-6.0)	-	
CDAI	-	-	186.0 (128.0-358.0)	
DAIBD	-	-	-	
Hb, g/dL, median (range)	14.6 (13.2-15.2)	14.1 (12.5-16.5)	12.7 (10.6-16.0)	0.17
ESR, mm/hr, median (range)	7.5 (3.0-24.0)	9.0 (2.0-45.0)	47.0 (17.0-99.0)	0.02
CRP, mg/L, median (range)	2.3 (0.6-5.5)	1.0 (0.3-25.5)	18.6 (0.7-91.3)	0.10
Albumin, g/dL, median (range)	4.4 (4.1-4.4)	4.4 (4.1-4.8)	3.7 (3.6-4.4)	0.10
Creatinine, mg/dL, median (range)	0.76 (0.62-0.99)	0.78 (0.56-0.94)	0.67 (0.61-0.95)	0.92
ALT, U/L, median (range)	14.0 (12.0-14.0)	11.0 (9.0-20.0)	10.0 (10.0-12.0)	0.71
Medication, n (%)				
5-ASA	-	9 (100)	4 (80.0)	0.36†
Steroid	-	2 (22.2)	1 (20.0)	1.00†
IMM	-	0	4 (80)	0.01†
Anti-TNF	-	0	0	-

	Plasma metabolite analysis (n=100)				*p*
Characteristics	Control (n=25)	UC (n=24)	CD (n=26)	BD (n=25)	
Age, median (range)	33.7 (26.0-43.6)	37.9 (18.0-68.6)	23.3 (18.0-42.6)	44.3 (23.3-62.9)	<0.001
Sex, male/female, n (%)	8 (32.0)/17 (68.0)	15 (62.5)/9 (37.5)	22 (84.6)/4 (15.4)	14 (56.0)/11 (44.0)	<0.01
BMI, kg/m^2, median (range)	21.8 (18.1-24.2)	21.8 (16.1-28.7)	20.6 (13.9-31.2)	21.5 (16.5-24.7)	0.53
Bowel resection history, n (%)	0	0	1 (3.8)	3 (12.0)	0.31
Disease duration, months, median (range)	-	32.1 (1.0-155.0)	7.2 (0-128.0)	5.9 (0-110.0)	<0.01†
Disease location, n (%)					

E1 (proctitis)	-	7 (29.2)	-	-	
E2 (left sided)	-	5 (20.8)	-	-	
E3 (pancolitis)	-	12 (50.0)	-	-	
L1 (ileal)	-	-	4 (15.4)	-	
L2 (colonic)	-	-	2 (7.7)	-	
L3 (ileocolic)	-	-	20 (76.9)	-	
With/without systemic BD, n (%)	-	-	-	16(64.0)/9(36.0)	
Disease activity, remission/mild/ moderate/severe, n (%)	-	4 (16.7)/11 (45.8)/4 (16.7)/5 (20.8)	8 (30.8)/10 (38.5)/8 (30.8)/0	6 (24.0)/ 6 (24.0)/7 (28.0)/6 (24.0)	0.08
Disease activity score, median (range)					
Partial Mayo score	-	3.5 (1.0-9.0)	-	-	
CDAI	-	-	184.5 (71.0-366.0)	-	
DAIBD	-	-	-	40.0 (10.0-150.0)	
Hb, g/dL, median (range)	12.4 (11.7-13.1)	13.7 (9.7-15.2)	13.9 (10.0-16.9)	12.5 (6.5-15.3)	0.52
ESR, mm/hr, median (range)	-	14.0 (2.0-84.0)	21.0 (7.0-119.0)	37.0 (2.0-120.0)	0.02†
CRP, mg/L, median (range)	-	1.0 (0.1-9.2)	6.5 (0.9-66.2)	2.4 (0.3-28.4)	<0.01†
Albumin, g/dL, median (range)	4.5 (4.4-4.6)	4.4 (3.5-5.1)	4.1 (3.4-4.8)	4.2 (3.4-5.1)	0.07
Creatinine, mg/dL, median (range)	0.7 (0.6-0.8)	0.7 (0.5-1.2)	0.7 (0.5-1.1)	0.8 (0.5-1.2)	0.34
ALT, U/L, median (range)	19 (17.0-21.0)	11.0 (5.0-34.0)	13.0 (5.0-47.0)	14.0 (6.0-58.0)	0.10
Medication, n (%)					
5-ASA	-	24 (100)	24 (92.3)	25 (100)	0.33†
Steroid	-	6 (25.0)	6 (23.1)	13 (52.0)	0.05†
IMM	-	7 (29.2)	15 (57.7)	7 (28.0)	0.05†
Anti-TNF	-	1 (4.2)	1 (3.8)	2 (8.0)	0.84†

UC: ulcerative colitis, CD: Crohn's disease, BD: Behçet's disease, SD: standard deviation, BMI: body mass index, CDAI: Crohn's disease activity index, DAIBD: disease activity index for intestinal Behçet's disease, CRP: C-reactive protein, ALT: alanine aminotransferase, 5-ASA: 5-aminosalicylic acid, IMM: immunomodulator, anti-TNF: anti-tumor necrosis factor

†*p* values were calculated between disease groups excluding the control group

2. Changes in microbiome in IBD and intestinal BD

A. Changes in tissue and fecal microbiota composition in IBD and intestinal BD

Among 73 tissue samples, 49 samples (6 samples in control group, 15 samples in UC, and 14 samples in CD and BD each) were sequenced targeting V1-3 region, whereas 24 samples (6 samples in control group and 9 samples in UC and BD each), which were collected later, were sequenced targeting V3-4 region. To investigate the differences in microbial composition in IBD and intestinal BD, the relative abundance of multiple taxa between control and IBD or intestinal BD was compared by the Mann–Whitney *U* test. In the phylum level, IBD and intestinal BD showed an increased tendency of Proteobacteria and Fusobacteria and a decreased tendency of Bacteroidetes compared with control (Figure 3). Increased Fusobacteria in UC compared with control was significant ($p < 0.05$). UC showed an increased abundance of order *Fusobacteriales*, family *Fusobacteriaceae* and *Burkholderiaceae,* and genus *Ralstonia* and *Fusobacterium*, whereas the genus *Roseburia* decreased. CD showed an increased abundance of order *Enterobacterales* and family *Enterobacteriaceae* and genus *Escherichia* and a decreased abundance of family *Ruminococcaceae* and *Coriobacteriaceae*, genus *Blautia, Anaerostipes, Faecalibacterium,* and *Roseburia*. In intestinal BD, a decreased abundance of family *Bacteroidaceae* and genus *Bacteroides, Acinetobacter*, and *Subdoligranulum* was noted, but these changes were only significant compared with control, and there was no significant change compared with IBD.

Microbial analysis of fecal samples of control and IBD showed similar but different patterns. At the phylum level, IBD showed decreased Firmicutes and Actinobacteria,

whereas Proteobacteria and Bacteroidetes increased compared with control (Figure 4). Microbial richness and evenness were evaluated by Shannon index, and tissue sample showed a significant decrease in the α-diversity in CD compared with control, UC, or BD (Figure 5). On fecal sample analysis, the Shannon index was not different in UC and CD, but the number of OTUs and phylogenetic diversity was decreased in UC compared with control. Beta-diversity analysis was performed by the Bray-Curtis method, and PCoA plot with tissue samples showed clustering according to groups, and significantly different microbial composition among control and CD (PERMANOVA *p* value = 0.011), UC and CD (PERMANOVA *p* value = 0.004), UC and BD (PERMANOVA *p* value = 0.01), and CD and BD (PERMANOVA *p* value = 0.002) was noted (Figure 6A). The PCoA plot with fecal samples showed more separation of IBD from control, and significantly different microbial composition among control and UC (PERMANOVA *p* value = 0.002) and control and CD (PERMANOVA *p* value = 0.025) (Figure 6B).

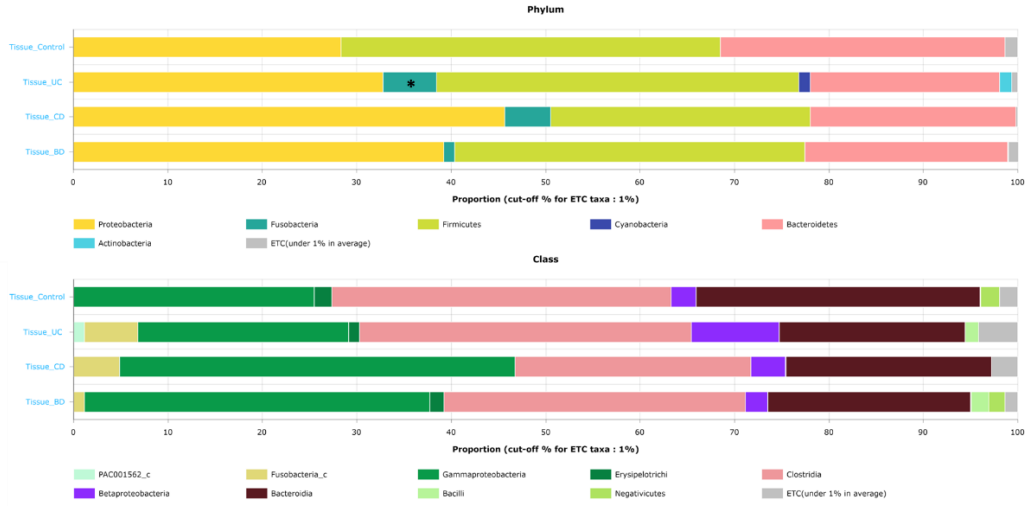

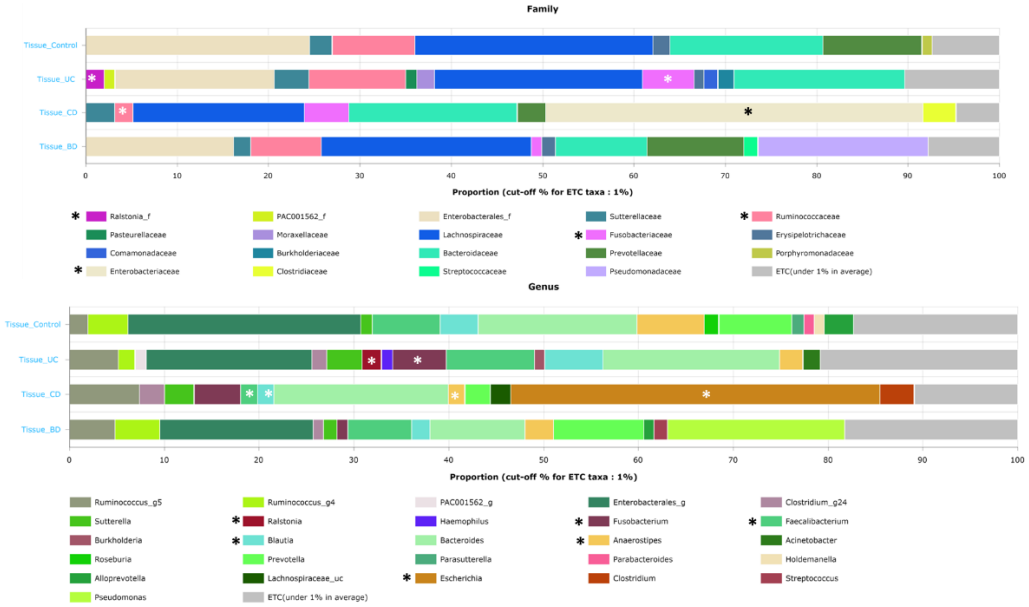

Figure 3. Stacked bar chart of the microbial composition of colon tissue.

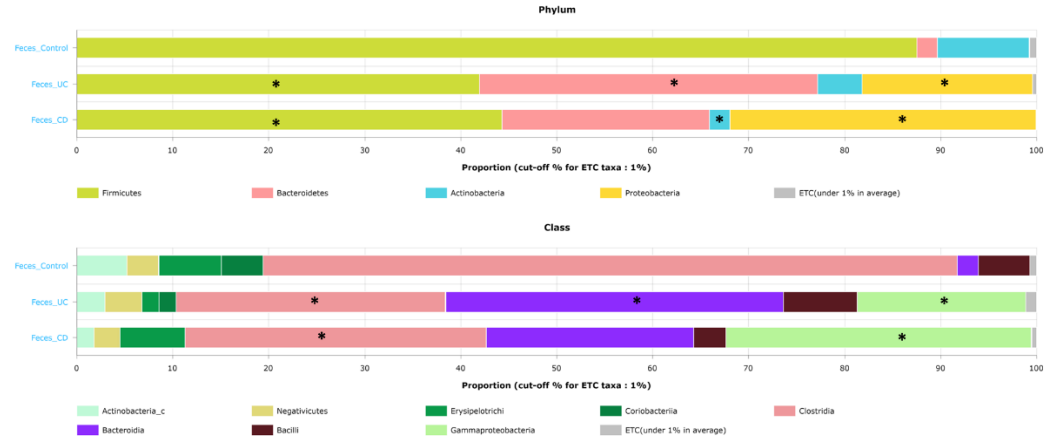

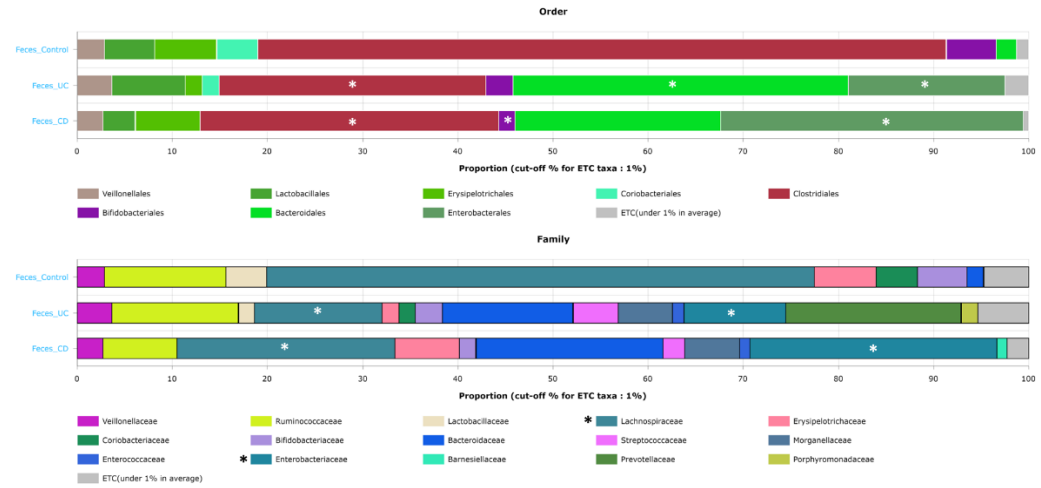

Figure 4. Stacked bar chart of the microbial composition of feces.

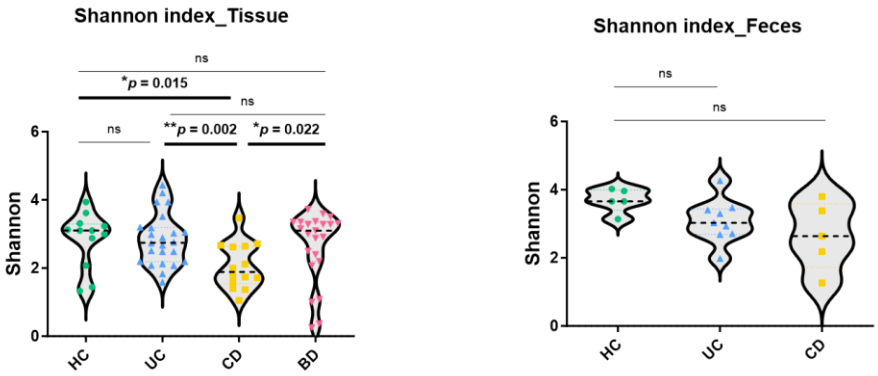

Figure 5. Microbial α-diversity index from tissue and fecal samples. Microbial richness and evenness were evaluated by the Shannon index, and the tissue sample showed a significant decrease in the α-diversity in CD compared with control, UC, or BD. CD: Crohn's disease, UC: ulcerative colitis, BD: Behçet's disease

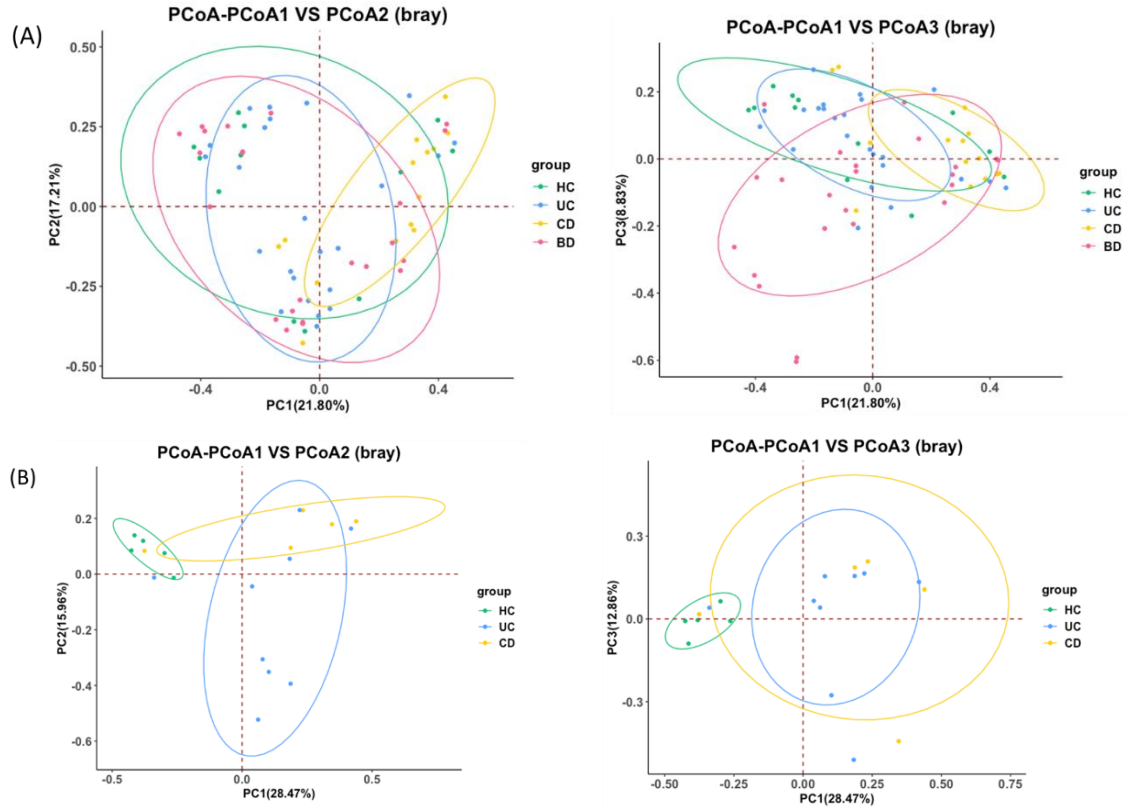

Figure 6. Principal coordinate analysis (PCoA) plot of tissue samples (A) and stool samples (B). Beta-diversity was analyzed by the Bray-Curtis method. (A) PCoA plot with tissue samples showed clustering according to groups, and significantly different microbial composition among control and CD, UC and CD, UC and BD, and CD and BD (all *p* value < 0.05). (B) PCoA plot with fecal samples showed more separation of IBD from control, and significantly different microbial composition among control and UC and control and CD (all $p < 0.05$). HC: healthy control, UC: ulcerative colitis, CD: Crohn's disease, BD: Behçet's disease

B. Taxonomic biomarker evaluation

LEfSe analysis of tissue samples demonstrated significantly different abundances of specific taxa between control, UC, CD, and BD, and taxa with LDA effect size > 3 and *p*

<0.05 were visualized in Figure 7A. In control group, class Coriobacteriia, order *Coriobacteriales* and *Bifidobacteriales*, family *Coriobacteriacea* and *Bifidobacteriaceae*, and genus *Roseburia, Holdemanella, Subdoligranulum, Fusicatenibacter, Bifidobacterium*, and *Barnesiella* were more abundant taxa than UC, CD, or BD, which can be a potential biomarker of discriminating healthy status versus IBD or intestinal BD. In UC, phylum Fusobacteria, class Alphaproteobacteria, Actinomycetia, Fusobacteriia, and Betaproteobacteria, order *Xanthomonadales, Rhizobiales*, and *Fusobacteriales,* family *Lactobacillaceae, Xanthomonadaceae, Comamonadaceae, Ralstonia, Burkholderiaceae, Fusobacteriaceae*, and *Ruminococcaceae*, genus *Lactobacillus, Dyella, Comamonas, Paraburkholderia, Ralstonia,* and *Fusobacterium* were differentially abundant taxa compared with control, CD, or BD. In CD, family *Morganellaceae*, genus *Proteus,* and *Escherichia* were more abundant than control, UC, or BD. In intestinal BD, genus *Lachnospira* was the only taxon with a valid name that was differentially abundant compared with control and IBD by LEfSe analysis.

LEfSe analysis separately performed for intestinal BD vs. control showed decreased abundance of butyrate-producing bacteria such as *Dorea formicigenerans, Subdoligranulum variabile, Roseburia ceciola, Coprococcus comes,* and *Caproiciproducens* (Figure 7B). LEfSe analysis of fecal samples also demonstrated significantly different abundances of specific taxa between the tissue of control, UC, and CD (Figure 7C). However, conducting a simultaneous LEfSe analysis for all four groups may not effectively capture taxa that are consistently increased or decreased across groups, as it tends to highlight features unique to a single group. To identify taxa that are commonly increased or decreased in UC, CD, and BD, we conducted separate LEfSe analyses for control vs. UC, control vs. CD, and control vs. intestinal BD. From these analyses, taxa that showed differences (LDA > 2.5, $p < 0.05$) were further assessed using the Mann-Whitney *U* test, and only those taxa with significant taxonomic composition changes by Mann-Whitney *U* test were selected as microbial biomarkers and visualized in a Venn diagram (Figure 8). Genus *Fusicatenibacter*, species *Fusicatenibacter saccharivorans,*

Coprococcus comes, Blautia obeum, *Dorea formicigenerans,* and *Roseburia ceciola* consistently exhibited decreased abundance, indicating their 'protective' role in UC, CD, and BD. UC exhibited the most dynamic changes, with many both increased and decreased taxa, while CD primarily showed a decrease in the abundance of multiple taxa. Intestinal BD, on the other hand, displayed fewer significant changes, mainly characterized by a decrease in the abundance of several taxa including *Subdoligranulum variabile* and *Blautia wexlerae*. As a specific alteration unique to intestinal BD, a decrease in the genus *Bacteroides*, particularly the species *Bacteroides fragilis*, was identified.

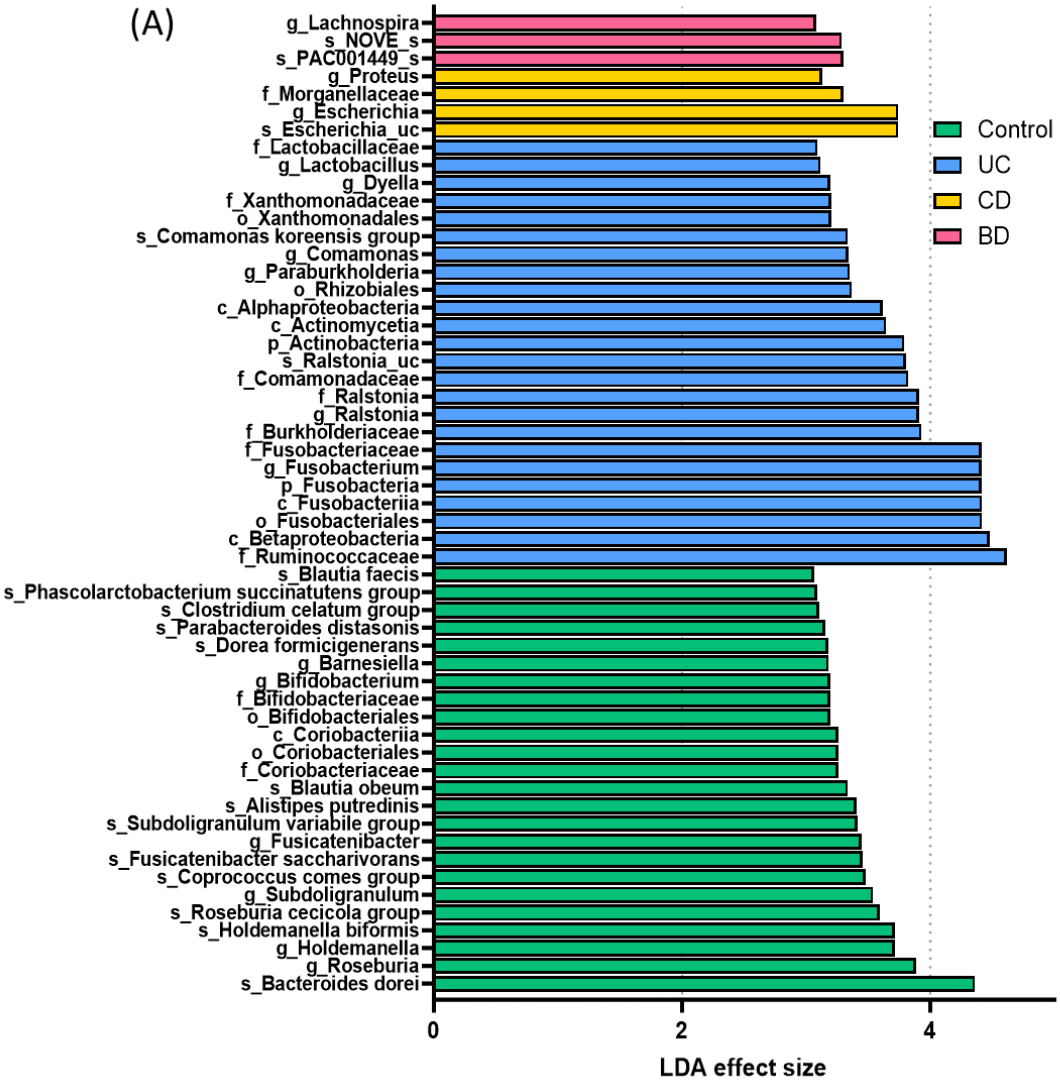

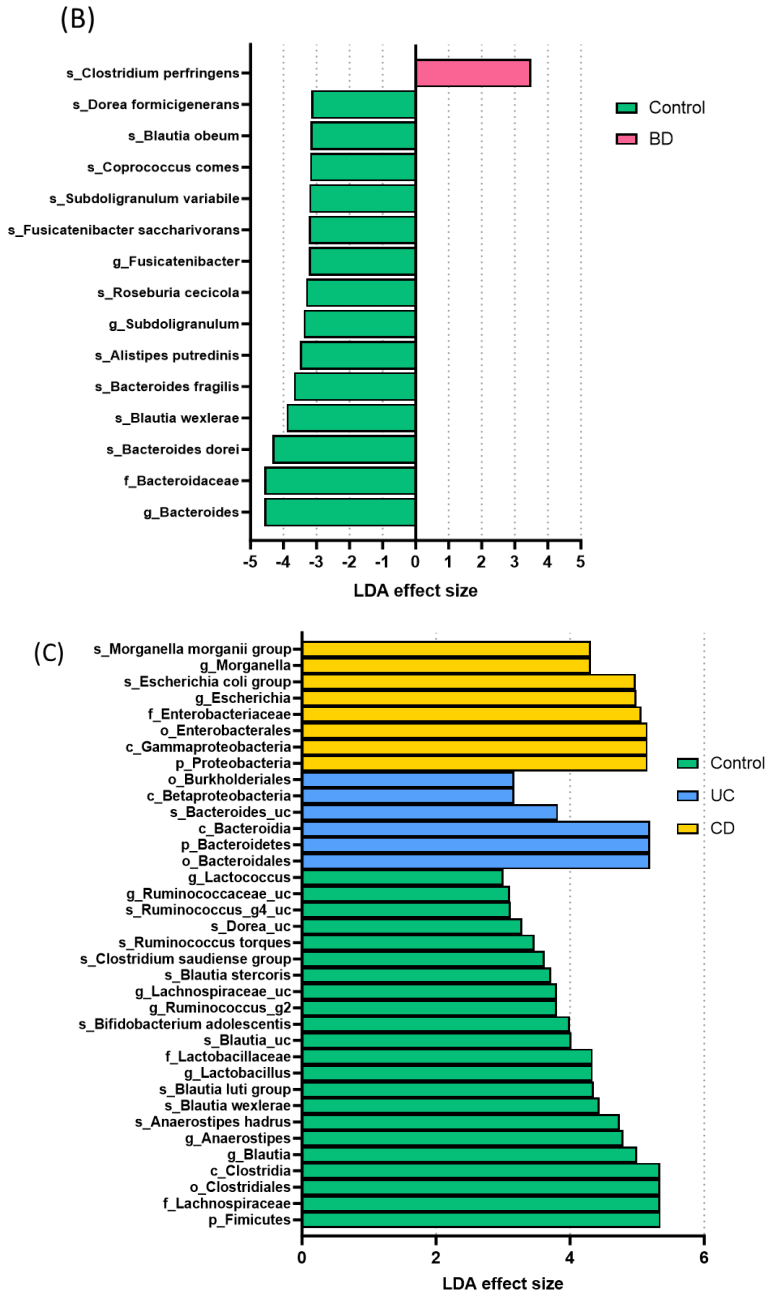

Figure 7. Taxonomic biomarkers analyzed by LEfSe of tissue samples (A, B) and fecal samples (C). Taxa with LDA effect size > 3 and p <0.05 were visualized. (A) LEfSe

analysis of tissue samples demonstrated significantly different abundances of specific taxa between control, UC, CD, and BD. (B) LEfSe analysis separately performed for intestinal BD vs. control showed a decreased abundance of butyrate-producing bacteria. (C) LEfSe analysis of fecal samples also demonstrated significantly different abundances of specific taxa between the tissue of control, UC, and CD. LDA: linear discriminant analysis, LEfSe: LDA effect size, UC: ulcerative colitis, CD: Crohn's disease, BD: Behçet's disease

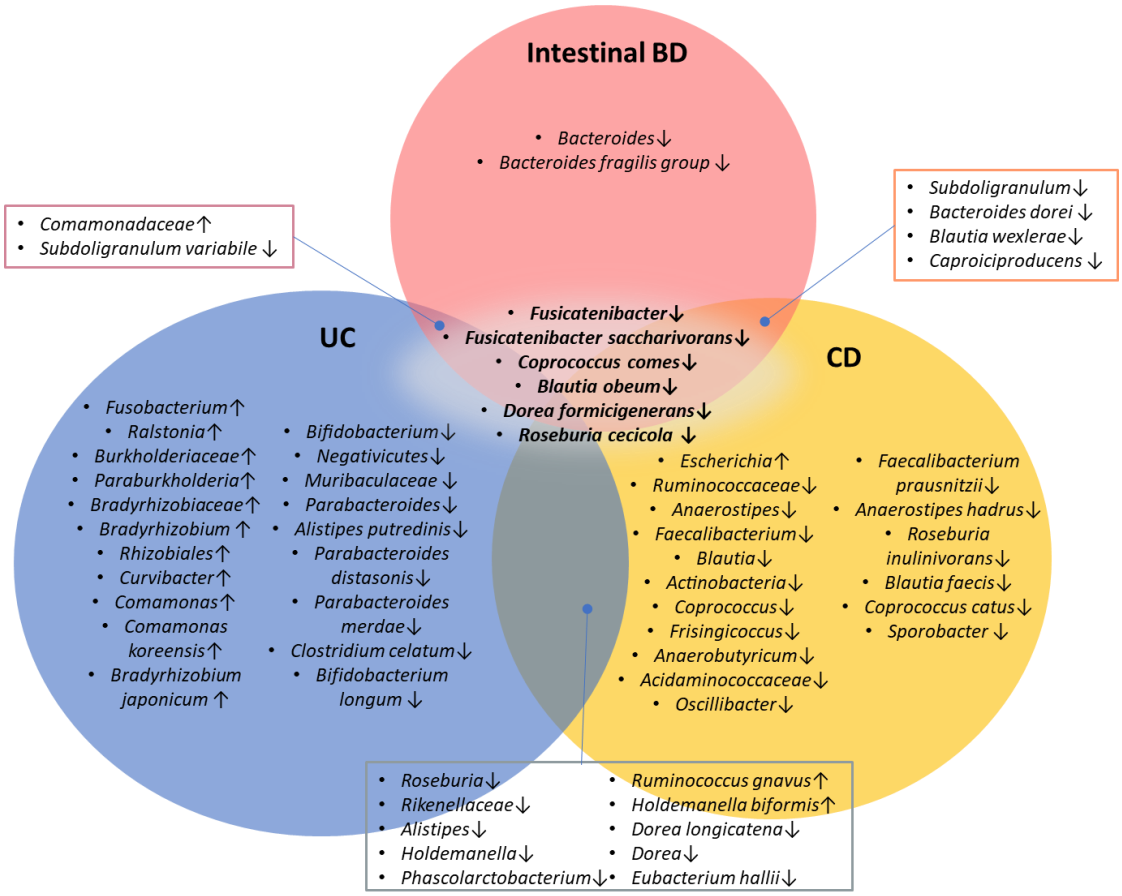

Figure 8. Microbial taxonomic biomarkers of IBD and intestinal BD. Genus *Fusicatenibacter*, species *Fusicatenibacter saccharivorans*, *Coprococcus comes*, *Blautia obeum*, *Dorea formicigenerans*, and *Roseburia ceciola* consistently exhibited decreased

abundance, indicating their 'protective' role in UC, CD, and BD. BD displayed fewer significant changes, mainly characterized by a decrease in the abundance of several taxa. IBD: inflammatory bowel disease, UC: ulcerative colitis, CD: Crohn's disease, BD: Behçet's disease

C. Predictive functional profiling of microbiome

Based on 16S rRNA gene sequencing data from tissue samples, we performed predictive functional profiling of the microbiome by PICRUSt analysis annotated to KEGG orthologys (KOs). In total, gene allocation for 42 KOs (2 in control, 11 in UC, 10 in CD, and 19 in BD) was differentially enhanced between groups with significance (LDA > 2.0, p <0.05, FDR-adjusted p < 0.1) (Figure 9). PICRUSt analysis from the microbiome of fecal samples showed no KOs, pathways, or modules with FDR-adjusted p < 0.1. Intestinal BD exhibited pronounced functional changes including orthologys related to drug resistance, signaling and cellular processes, as well as metabolic pathways.

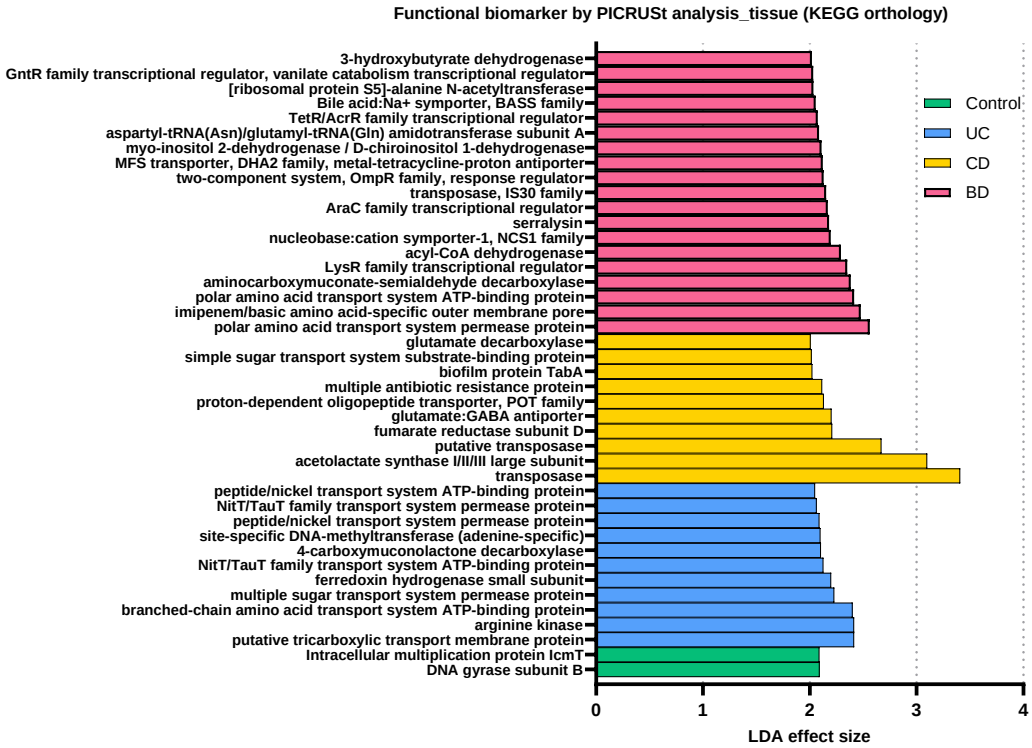

Figure 9. Predictive functional profiling based on PICRUSt analysis (KEGG orthology) from tissue samples. PICRUSt analysis revealed multiple enhanced gene allocations for each group. Intestinal BD exhibited pronounced enhancements in functions related to drug resistance, signaling and cellular processes, as well as metabolic pathways. PICRUSt: phylogenetic investigation of communities by reconstruction of unobserved states, KEGG: Kyoto Encyclopedia of Genes and Genomes, UC: ulcerative colitis, CD: Crohn's disease, BD: Behçet's disease

3. Metabolomic analysis

A. GC-TOF-MS analysis

(1) Changes in metabolite between groups

GC-TOF-MS metabolomic analysis of 100 individual samples (25 Control, 24 UC, 26 CD, and 25 BD) was performed. In the PCA score plots, control and UC formed one cluster, while CD and BD constituted another distinct cluster. The PLS-DA score plot derived from the value of the PCA model demonstrated the segregation of three groups: control, UC, and a combined group of CD and BD (Figure 10A, B). Despite the observed significant difference among the three clusters ($p < 0.05$), the reproducibility and predictability were limited ($R^2 = 0.43$, $Q^2 = 0.30$), and a clear separation between CD and BD was not achieved. Consequently, a 3D PLS-DA score plot was constructed, which exhibited distinct separation among all four groups (Figure 10C). The PLS-DA cross-validation data showed cumulative values of $R^2 = 0.61$ and $Q^2 = 0.52$ where R^2 indicates the variation shown by all 5 components in the model and Q^2 shows the predictability when the 5 components were considered (Figure 10D). These score plots and values indicated good clustering and demonstrated a good distinction between the four groups. Subsequently, we employed this model to identify the metabolites contributing to the group differentiation. The whole metabolomics profiles are shown as heatmap (Figure 11). Correlation analysis by Spearman rank correlation between metabolites is shown in the correlation heatmap (Figure 12). Metabolites within the same categories, such as fatty acids or amino acids, exhibited a positive correlation within each category.

The key metabolites that contributed most to the separation between controls, UC, CD, and BD are shown in a PLS-DA VIP plot, ranking these by importance (Figure 13). VIP scores rank the overall contribution of each variable to the PLS-DA model. Uracil showed as a top metabolite in the discriminant analysis with higher levels in UC, lower levels in CD and BD, and intermediate levels in control. The following top metabolites oleamide, glutamine, glycerol-3-phosphate, hydroxylamine, oxalic acid, glucose, 2-oxoglutaric acid, glycerol, cysteine showed similar patterns of decreasing in UC and increasing in CD and BD.

(A)

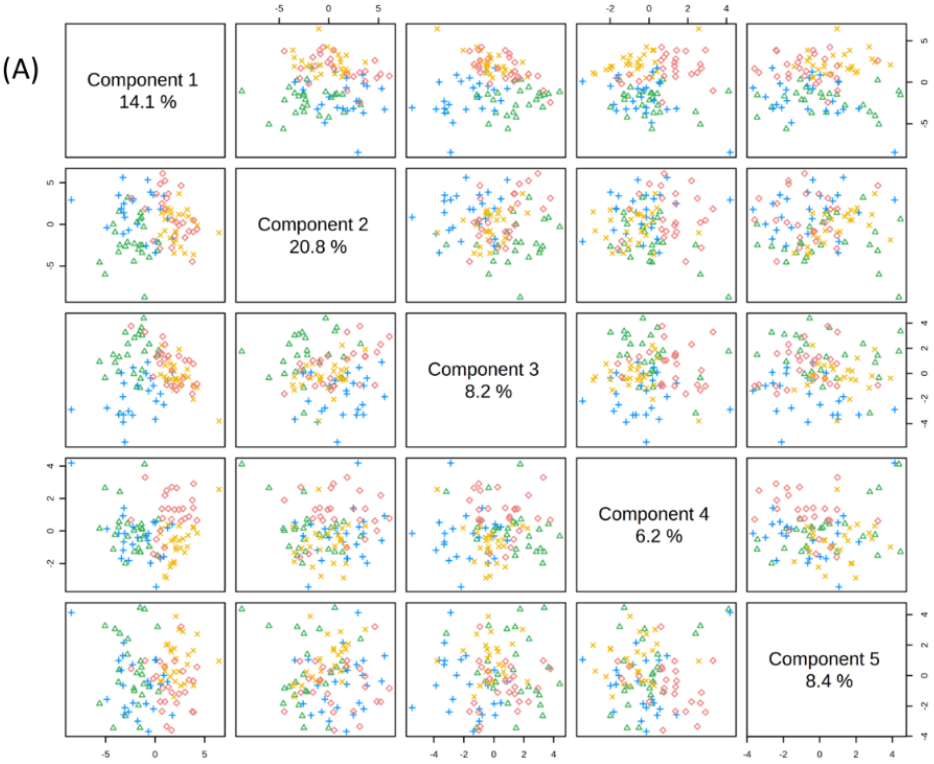

(B)

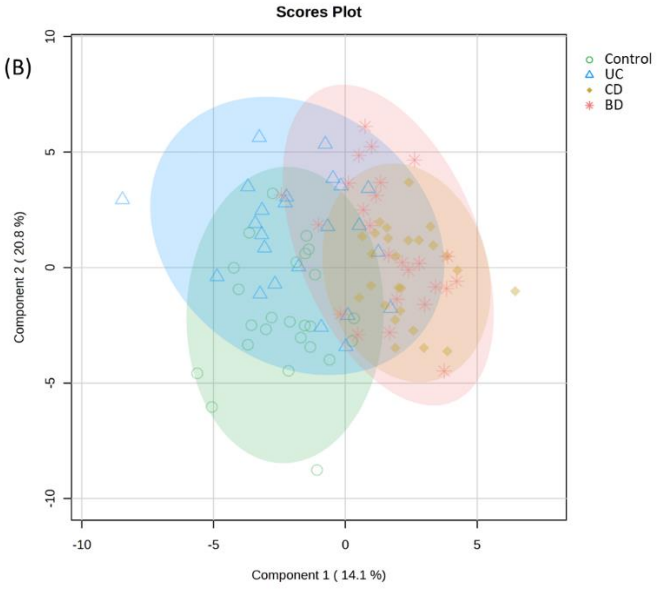

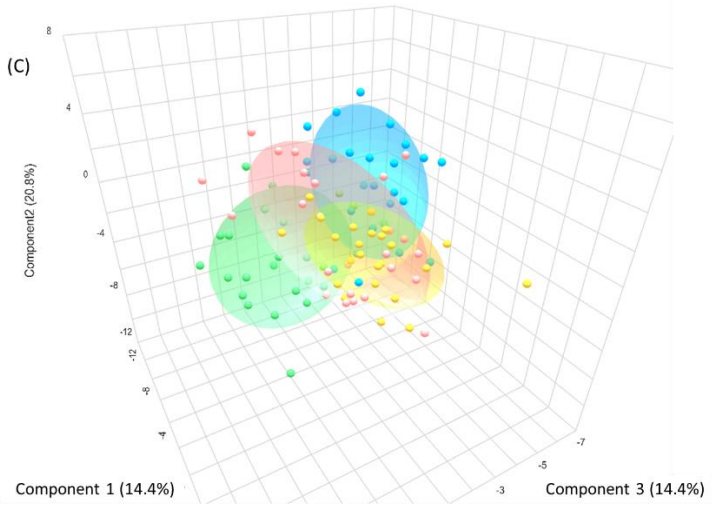

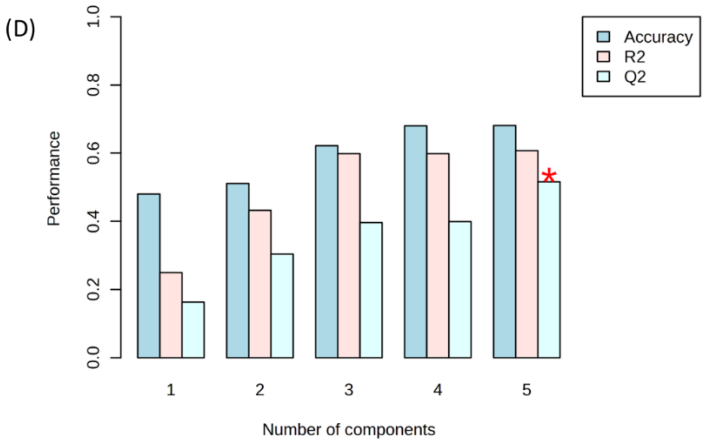

Figure 10. Partial least squares discriminant analysis (PLS-DA) of plasma metabolites by GC-TOF-MS analysis. (A) Using a total of five components, we can identify combinations of two components that best explain the differences between groups. Figure-wise, it is evident that components 1 and 2 exhibit high explanatory power and effectively illustrate the differences between groups. (B) PLS Score 2D Plot generated using components 1 and 2. The plot demonstrated the segregation of three groups: control, UC, and a combined group of CD and BD. (C) PLS Score 3D Plot using components 1, 2, and 3. (D) PLS-DA cross-validation showed cumulative values of $R^2 = 0.61$ and $Q^2 = 0.52$ where R^2 indicates

the variation shown by all 5 components in the model. GC-TOF-MS: gas chromatography time-of-flight mass spectrometry, UC: ulcerative colitis, CD: Crohn's disease, BD: Behçet's disease

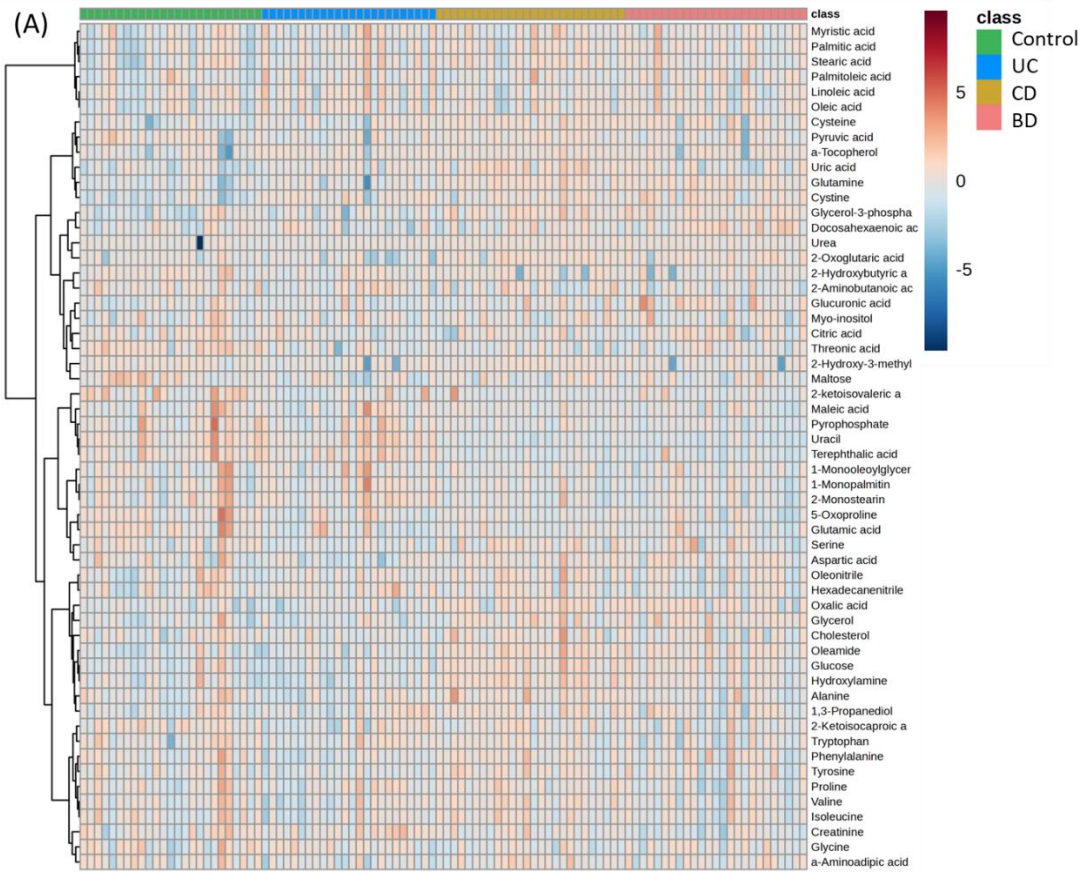

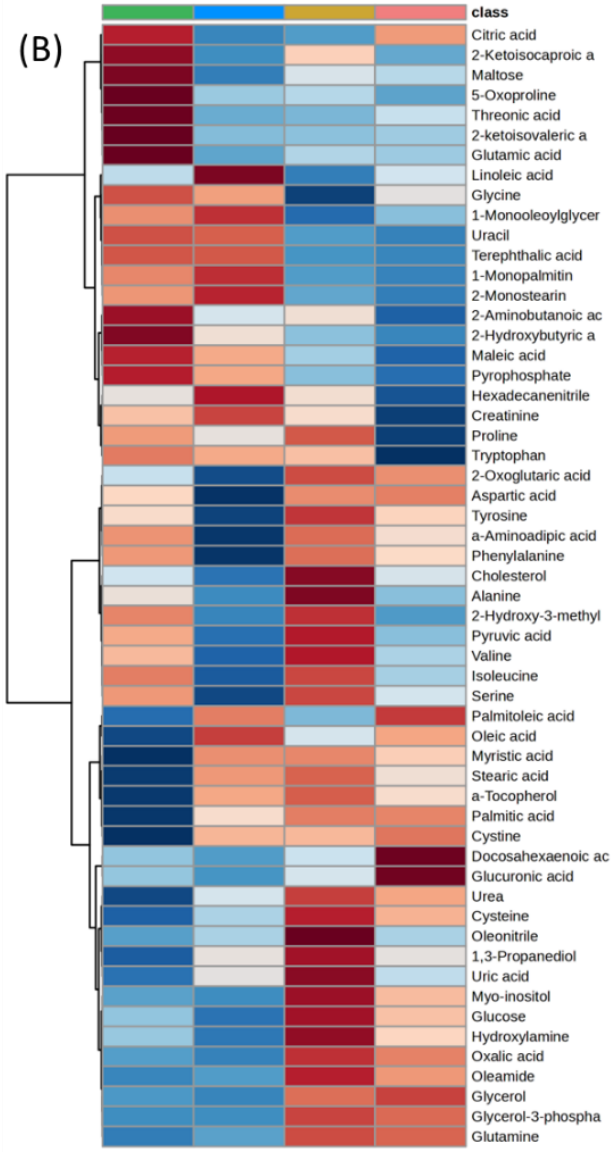

Figure 11. Heatmap of the whole plasma metabolite profiles by individual samples (A) and by groups (B). Overall, the metabolite profiles showed a similarity between control and UC, and a similarity between CD and BD. UC: ulcerative colitis, CD: Crohn's disease, BD: Behçet's disease

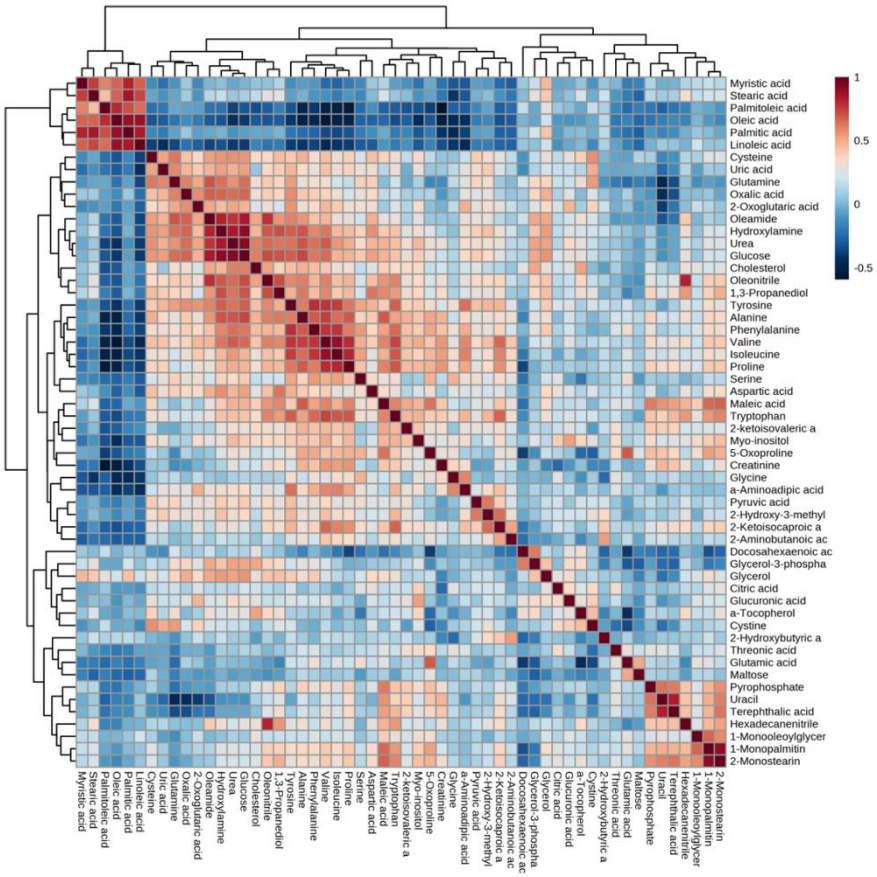

Figure 12. Correlation analysis between metabolites. A correlation heatmap by Spearman rank correlation analysis is shown. Metabolites within the same categories, such as fatty acids or amino acids, exhibited a positive correlation within each category.

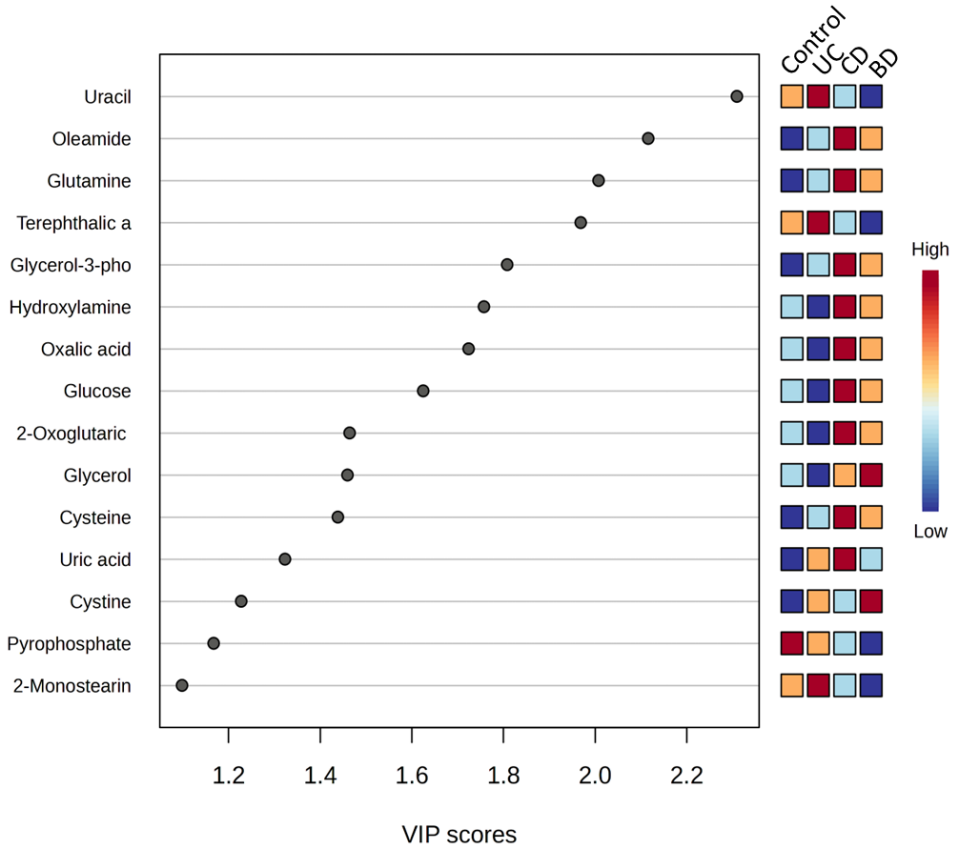

Figure 13. Plasma partial least squares discriminant analysis (PLS-DA) variable importance in projection (VIP) plot. The key metabolites that contributed most to the separation between controls, UC, CD, and BD are shown in a PLS-DA VIP plot, ranking these by importance. UC: ulcerative colitis, CD: Crohn's disease, BD: Behçet's disease

(2) Metabolomic biomarker discovery

Among 56 metabolites on the heatmap, 26 metabolites with VIP >1.0 by five components of the selected PLS-DA model, $p < 0.05$, FDR $p < 0.1$ by ANOVA were identified and selected as metabolites that differed between control, UC, CD, and BD. These potential metabolomic biomarkers of IBD and intestinal BD are summarized as a Venn diagram (Figure 14, Table 2). There were common changes observed among the three groups

when compared to the control group. These common changes included an increase in cystine and a decrease in threonic acid, glutamic acid, 2-ketoisovaleic acid, and 5-oxoproline. Substantial overlap was also observed between intestinal BD and CD, characterized by a decrease in terephthalmic acid and uracil, as well as an increase in oleamide, glutamine, glycerol, glycerol-3-phosphate, oxalic acid, and cysteine. UC exhibited a distinct metabolite profile compared to the other two conditions, except for the shared alterations among the three groups. Notably, UC had the least pronounced metabolite changes compared to the control, with decreases in phenylalanine and maltose being the notable changes. In CD, a distinct increase in hydroxylamine, glucose, and uric acid was noted compared to the control and other groups. In BD, a distinct increase in glucuronic acid and a decrease in pyrophosphate were notably observed.

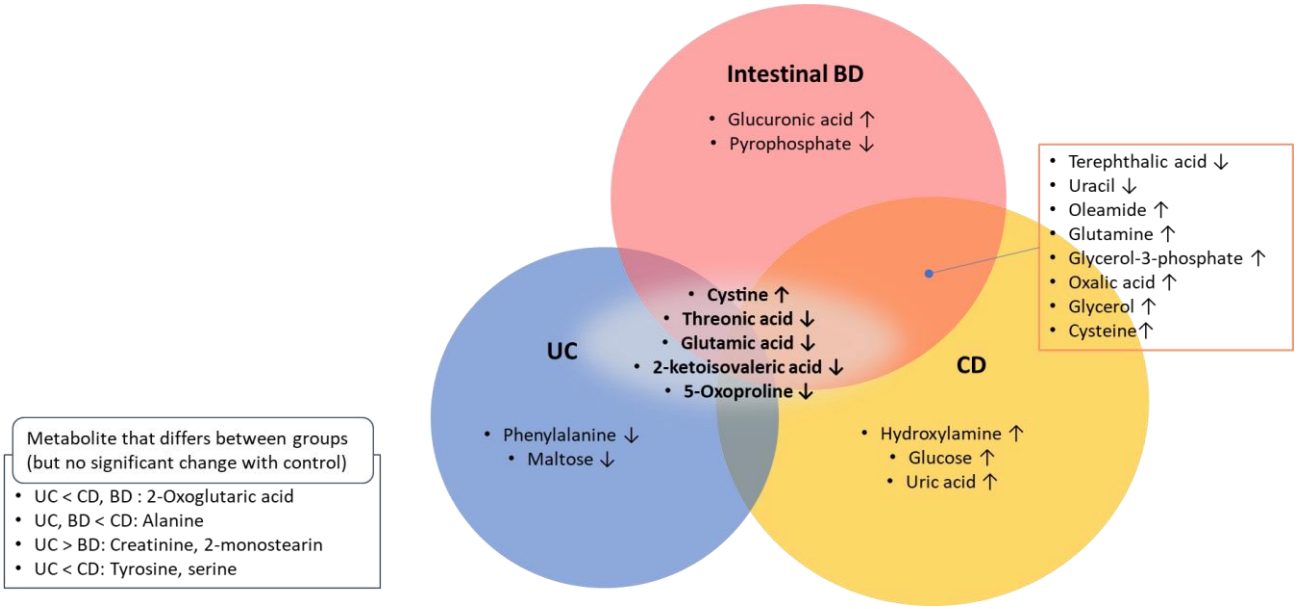

Figure 14. Potential metabolomic biomarkers of IBD and intestinal BD. In total, 26 metabolites with VIP > 1.0, ANOVA $p < 0.05$, and FDR-adjusted $p < 0.1$ (20 different with control, 6 different between UC, CD, and BD) were noted. IBD: inflammatory bowel disease, UC: ulcerative colitis, CD: Crohn's disease, BD: Behçet's disease, VIP: variable importance in projection, ANOVA: analysis of variance, FDR: false discovery rate

(3) Functional aspects of metabolomic biomarkers

To identify biologically meaningful patterns based on the metabolomics data, QEA was performed for all diseases collectively (control vs. IBD and intestinal BD) and separately for UC, CD, and intestinal BD. When comparing control and inflammatory diseases of bowel (UC, CD, and intestinal BD), 27 pathways including nitrogen metabolism, nucleotide metabolism, amino acid metabolism, lipid metabolism, carbohydrate metabolism, metabolism of cofactors and vitamins, and genetic information processing were enhanced (Table 3, Figure 15A). In UC, metabolic pathway analysis revealed 18 pathways that were significantly enriched compared to controls, with 11 of them related to amino acid metabolism (Figure 15B). In CD, 28 enriched metabolic pathways were identified (Figure 15C). In BD, 28 enriched pathways were identified, including 11 related to amino acid metabolism, 4 to lipid metabolism, 6 to carbohydrate metabolism, 3 to cofactor and vitamin metabolism, 1 to energy metabolism, 2 to nucleotide metabolism, and 1 to genetic information processing (Table 4, Figure 15D).

Table 2. List of significantly changed and differentially expressed between control, UC, and CD

Name	F-value	P value	FDR-adjusted *p* value	Tukey's post-hoc comparisons	Max VIP score
Uracil	23.304	<0.001	<0.001	2-0; 3-0; 2-1; 3-1	2.40
Oleamide	16.482	<0.001	<0.001	2-0; 3-0; 2-1; 3-1	2.12
Glutamine	14.065	<0.001	<0.001	2-0; 3-0; 2-1; 3-1	2.01
Terephthalic acid	13.91	<0.001	<0.001	2-0; 3-0; 2-1; 3-1	1.97

Hydroxylamine	13.181	<0.001	<0.001	2-0; 2-1; 3-1; 3-2	1.76
Glycerol-3-phosphate	10.593	<0.001	<0.001	2-0; 3-0; 2-1; 3-1	1.81
Cystine	10.317	<0.001	<0.001	1-0; 2-0; 3-0	1.51
Glucose	9.8479	<0.001	<0.001	2-0; 2-1; 3-1	1.62
Oxalic acid	9.5713	<0.001	<0.001	2-0; 3-0; 2-1; 3-1	1.72
Uric acid	9.5247	<0.001	<0.001	2-0; 2-1; 3-2	1.40
2-Oxoglutaric acid	9.1817	<0.001	<0.001	2-1; 3-1	1.46
Threonic acid	8.0659	<0.001	<0.001	1-0; 2-0; 3-0	1.38
Glycerol	6.6603	<0.001	0.0016873	2-0; 3-0; 2-1; 3-1	1.46
Cysteine	6.5862	<0.001	0.0017107	2-0; 3-0; 2-1	1.44
Glutamic acid	5.9269	<0.001	0.0035111	1-0; 2-0; 3-0	1.19
Glucuronic acid	5.2158	0.0022235	0.0077824	3-0; 3-1	1.11
Alanine	4.7845	0.0037665	0.012407	2-1; 3-2	1.05
2-ketoisovaleric acid	4.5695	0.0049041	0.015257	1-0; 2-0; 3-0	1.17
Phenylalanine	4.4673	0.0055614	0.015677	1-0; 2-1	1.17
Pyrophosphate	4.4619	0.0055988	0.015677	3-0	1.17
5-Oxoproline	4.3706	0.0062657	0.016709	1-0; 2-0; 3-0	1.10
Creatinine	4.2251	0.0074979	0.019086	3-1	1.27
2-Monostearin	3.8419	0.012051	0.027705	3-1	1.15
Maltose	3.821	0.012369	0.027705	1-0	1.08
Tyrosine	3.3493	0.022237	0.046122	2-1	1.09

Serine	3.2671	0.024636	0.049273	2-1	1.01

Among the 56 metabolites, 26 metabolites with VIP score > 1.0 by PLS-DA model with 5 components and $p < 0.05$, FDR-adjusted $p < 0.1$ by ANOVA are selected. For Tukey's post-hoc comparisons, 0 is control, 1 is UC, 2 is CD, and 3 is BD.

Table 3. Result from quantitative enrichment analysis of ulcerative colitis, Crohn's disease, and intestinal Behçet's disease compared with control

	Total compound	Hits	Statistic Q	Raw *p*	FDR-adjusted *p*
Pantothenate and CoA biosynthesis	19	5	7.91	<0.001	<0.001
Pyrimidine metabolism	39	2	14.66	<0.001	<0.001
Nitrogen metabolism	6	2	14.45	<0.001	<0.001
Glutathione metabolism	28	4	9.68	<0.001	<0.001
Purine metabolism	65	3	10.02	<0.001	<0.001
Cysteine and methionine metabolism	33	4	9.49	<0.001	<0.001
Arginine biosynthesis	14	5	6.88	<0.001	<0.001
D-Glutamine and D-glutamate metabolism	6	3	9.82	<0.001	<0.001
Glyoxylate and dicarboxylate metabolism	32	5	6.56	<0.001	<0.001
Butanoate metabolism	15	2	7.91	<0.001	0.001
beta-Alanine metabolism	21	2	7.90	<0.001	0.001
Porphyrin and chlorophyll metabolism	30	2	8.10	<0.001	0.001
Alanine, aspartate and glutamate metabolism	28	7	4.64	<0.001	0.002
Histidine metabolism	16	2	7.68	<0.001	0.003
Taurine and hypotaurine metabolism	8	1	10.84	<0.001	0.003
Thiamine metabolism	7	1	10.84	<0.001	0.003
Arginine and proline metabolism	38	3	5.49	0.002	0.005
Glycerolipid metabolism	16	2	6.82	0.002	0.007
Glycerophospholipid metabolism	36	1	8.58	0.003	0.008

Valine, leucine and isoleucine degradation	40	4	4.72	0.010	0.024
Valine, leucine and isoleucine biosynthesis	8	4	4.72	0.010	0.024
Aminoacyl-tRNA biosynthesis	48	12	3.78	0.010	0.024
Glycine, serine and threonine metabolism	33	3	4.08	0.012	0.025
Fatty acid elongation	38	1	6.09	0.013	0.027
Fatty acid degradation	39	1	6.09	0.013	0.027
Fatty acid biosynthesis	47	2	4.17	0.034	0.066
Biosynthesis of unsaturated fatty acids	36	4	3.56	0.049	0.090

Table 4. Result from quantitative enrichment analysis of intestinal Behçet's disease compared with control

	Total compound	Hits	Statistic Q	Raw *p*	FDR-adjusted *p*
Pyrimidine metabolism	39	2	41.42	<0.001	<0.001
beta-Alanine metabolism	21	2	22.32	<0.001	<0.001
D-Glutamine and D-glutamate metabolism	6	3	21.16	<0.001	<0.001
Pantothenate and CoA biosynthesis	19	5	14.23	<0.001	<0.001
Arginine biosynthesis	14	5	13.55	<0.001	<0.001
Nitrogen metabolism	6	2	27.86	<0.001	<0.001
Glycerolipid metabolism	16	2	20.82	<0.001	<0.001
Purine metabolism	65	3	15.84	<0.001	<0.001
Glycerophospholipid metabolism	36	1	25.60	<0.001	<0.001
Cysteine and methionine metabolism	33	4	13.58	<0.001	0.001
Glyoxylate and dicarboxylate metabolism	32	5	11.63	<0.001	0.001
Alanine, aspartate and glutamate metabolism	28	7	9.66	<0.001	0.001
Butanoate metabolism	15	2	12.27	0.001	0.01
Glutathione metabolism	28	4	10.62	0.002	0.01
Pentose and glucuronate interconversions	18	1	14.32	0.01	0.02
Arginine and proline	38	3	8.13	0.01	0.03

metabolism					
Porphyrin and chlorophyll metabolism	30	2	8.67	0.02	0.04
Taurine and hypotaurine metabolism	8	1	11.31	0.02	0.04
Thiamine metabolism	7	1	11.31	0.02	0.04
Histidine metabolism	16	2	8.76	0.02	0.04
Aminoacyl-tRNA biosynthesis	48	12	6.90	0.02	0.04
Galactose metabolism	27	3	7.26	0.03	0.04
Fatty acid elongation	38	1	8.99	0.03	0.07
Fatty acid degradation	39	1	8.99	0.03	0.07
Ascorbate and aldarate metabolism	8	2	7.21	0.04	0.07
Inositol phosphate metabolism	30	2	7.21	0.04	0.07
Valine, leucine and isoleucine degradation	40	4	6.43	0.04	0.07
Valine, leucine and isoleucine biosynthesis	8	4	6.43	0.04	0.07

(A)

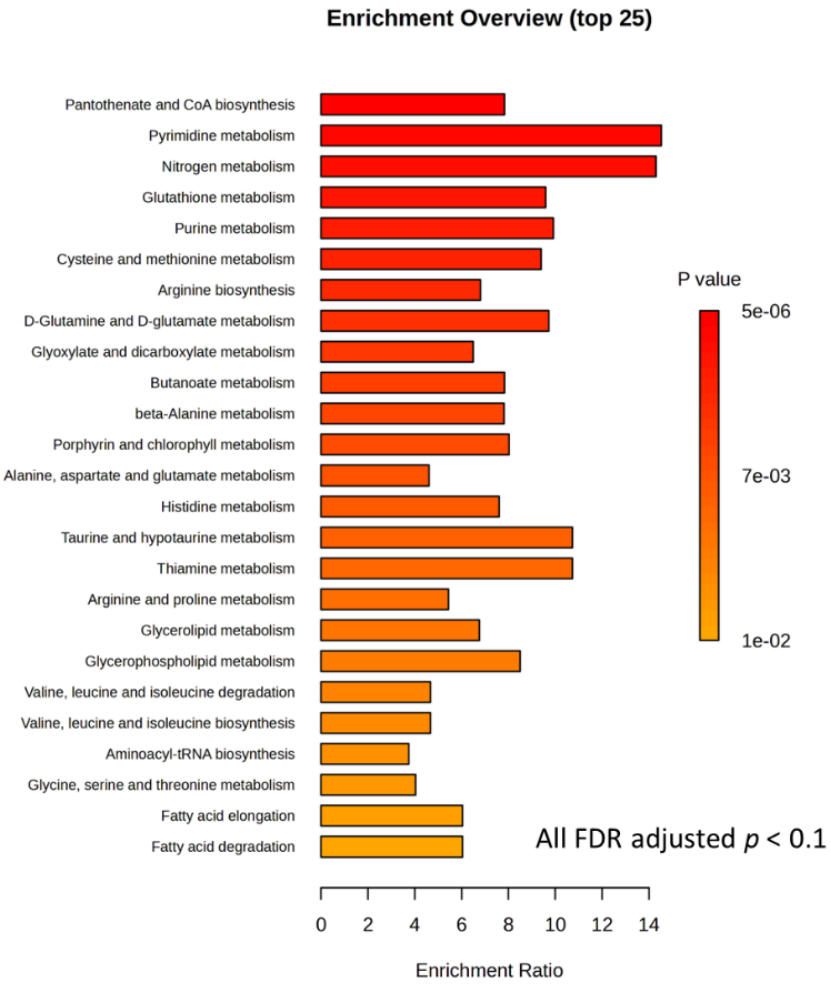

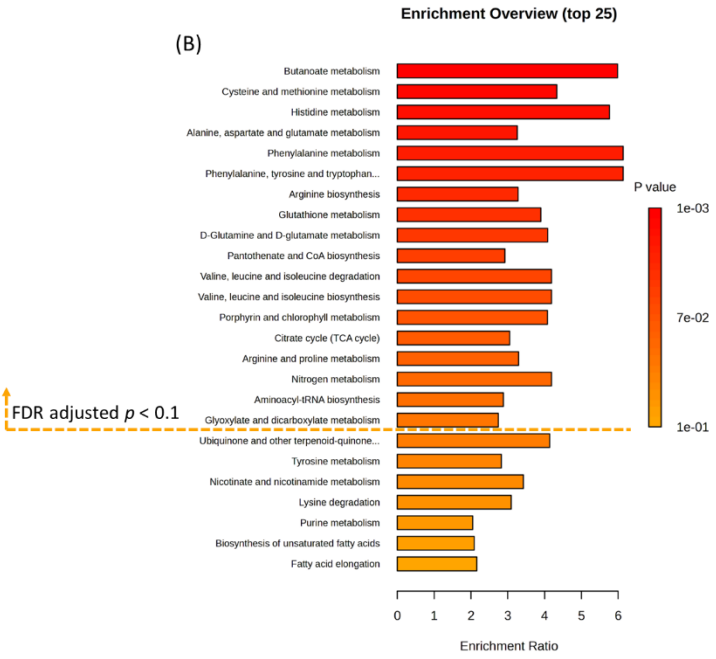

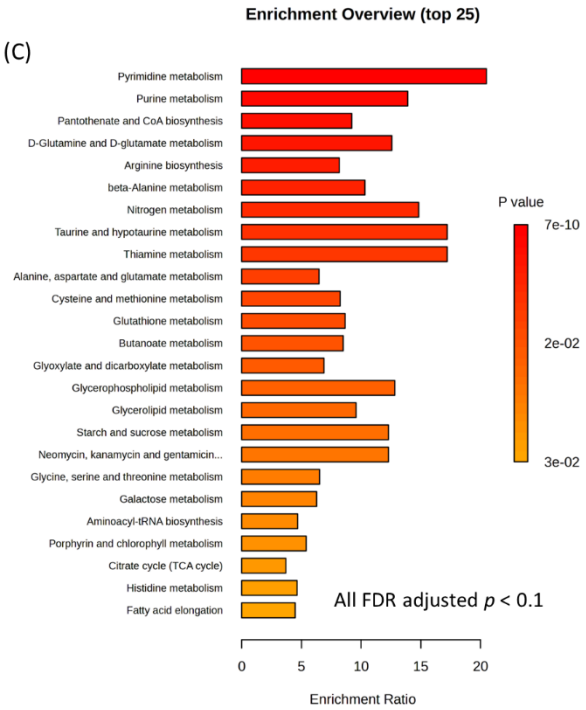

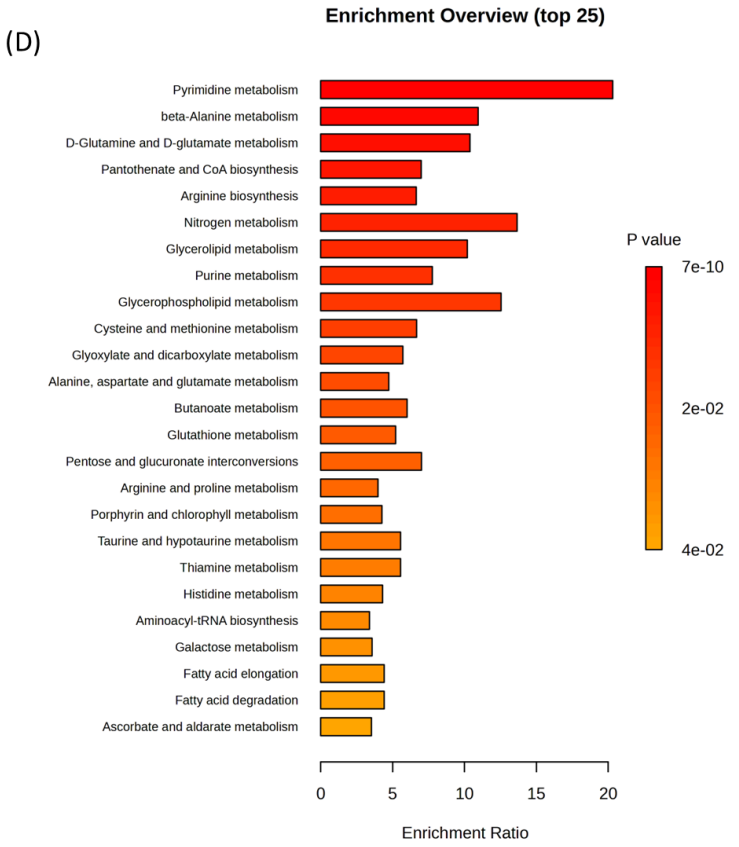

Figure 15. Quantitative enrichment analysis (QEA) for IBD and intestinal BD (A), UC (B), CD (C), and intestinal BD (D) compared with the control mapped to KEGG pathway (FDR-adjusted $p < 0.1$). IBD: inflammatory bowel disease, UC: ulcerative colitis, CD: Crohn's disease, BD: Behçet's disease, KEGG: Kyoto Encyclopedia of Genes and Genomes, FDR: false discovery rate

B. UPLC-Q-TOF-MS analysis

UPLC-Q-TOF-MS metabolomic analysis of 100 individual samples (25 Control, 24 UC, 26 CD, and 25 BD) was also performed, and 18 lysophospholipids including lysophosphatidylcholine (lysoPC) and lysophosphatidylethanolamine (lysoPE) were identified. However, these lysophospholipids did not show significant differentiation

between groups in both PCA score plots and PLS-DA score plots. The whole metabolomics profiles by UPLC-Q-TOF-MS analysis are shown as heatmap (Figure 16). Similar to the GC-TOF-MS analysis, a trend was observed where control and UC appeared similar, and BD and CD appeared similar. However, aside from the increase in lysoPE in CD, there were no specific trends.

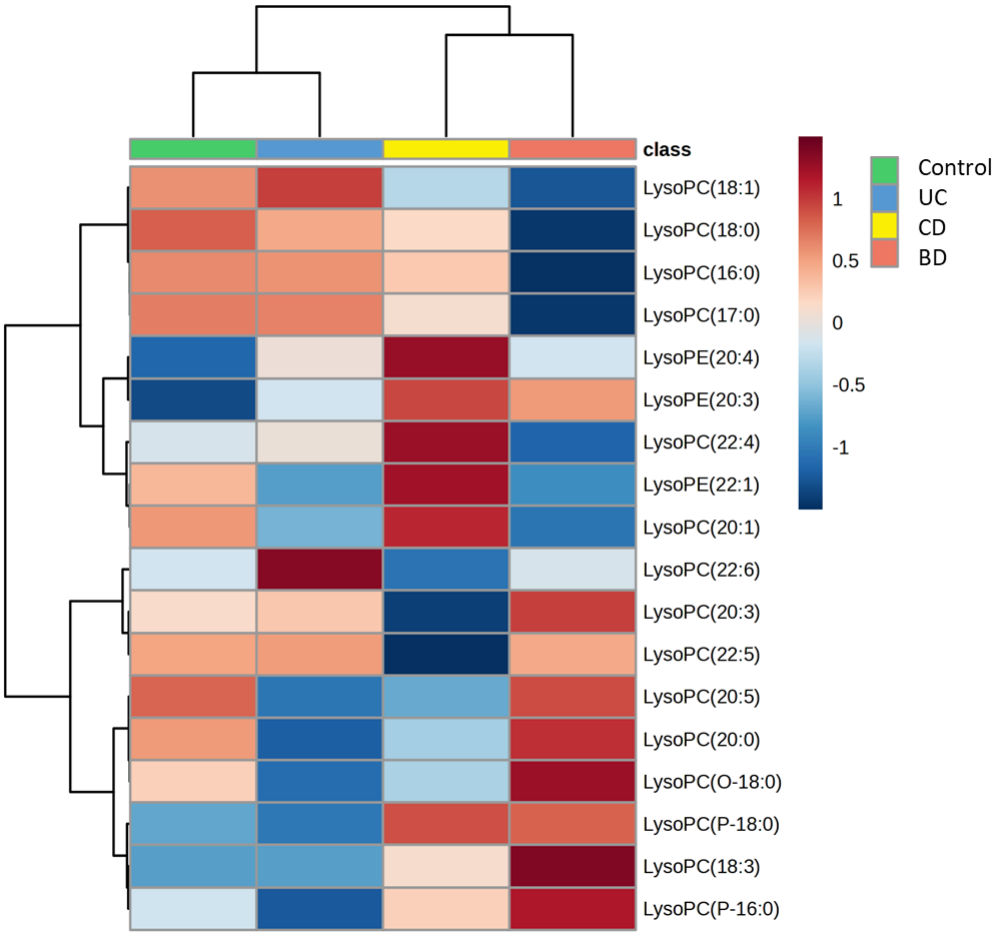

Figure 16. Heatmap of plasma metabolite profiles using UPLC-Q-TOF-MS analysis by groups. UPLC-Q-TOF-MS: ultra-performance liquid chromatography–quadrupole/time-of-flight mass spectrometry, UC: ulcerative colitis, CD: Crohn's disease, BD: Behçet's disease

4. Integration of microbial and metabolomic biomarkers

The correlation analysis by Spearman rank correlation between potential microbial and metabolomic biomarkers is shown in the correlation heatmap (Figure 17). Microbial taxa that are mainly decreased in UC show mostly positive correlations with the majority of metabolomic biomarkers, and this may be associated with the overall decrease in metabolites in UC. On the other hand, microbial taxa that are predominantly decreased in CD and BD exhibited a negative correlation with the majority of metabolomic biomarkers, resulting in an increase in metabolites in both CD and BD.

When comparing the enriched pathways from microbial functional analysis by PICRUSt and metabolite QEA, we observed a consistent pattern where microbial functions showed a good alignment with the enriched pathways identified by QEA. In UC, microbial functions of arginine kinase and branched-chain amino acid transport system ATP-binding protein were found to be increased, corresponding to enriched metabolite pathways arginine and proline metabolism and valine, leucine, and isoleucine degradation. In CD, microbial functions of acetolactate synthase I/II/III large subunit, fumarate reductase subunit D, and glutamate decarboxylase were found to be increased, corresponding to enriched metabolite pathways pantothenate and CoA biosynthesis, butanoate metabolism, citrate cycle, beta-alanine metabolism, taurine and hypotaurine metabolism, and alanine, aspartate, and glutamate metabolism. In BD, enriched metabolic pathways that showed correlation with PICRUSt results were pyrimidine metabolism, purine metabolism, alanine, aspartate, and glutamate metabolism, butanoate metabolism, arginine and proline metabolism, histidine metabolism, aminoacyl-tRNA biosynthesis, fatty acid degradation, and inositol phosphate metabolism.

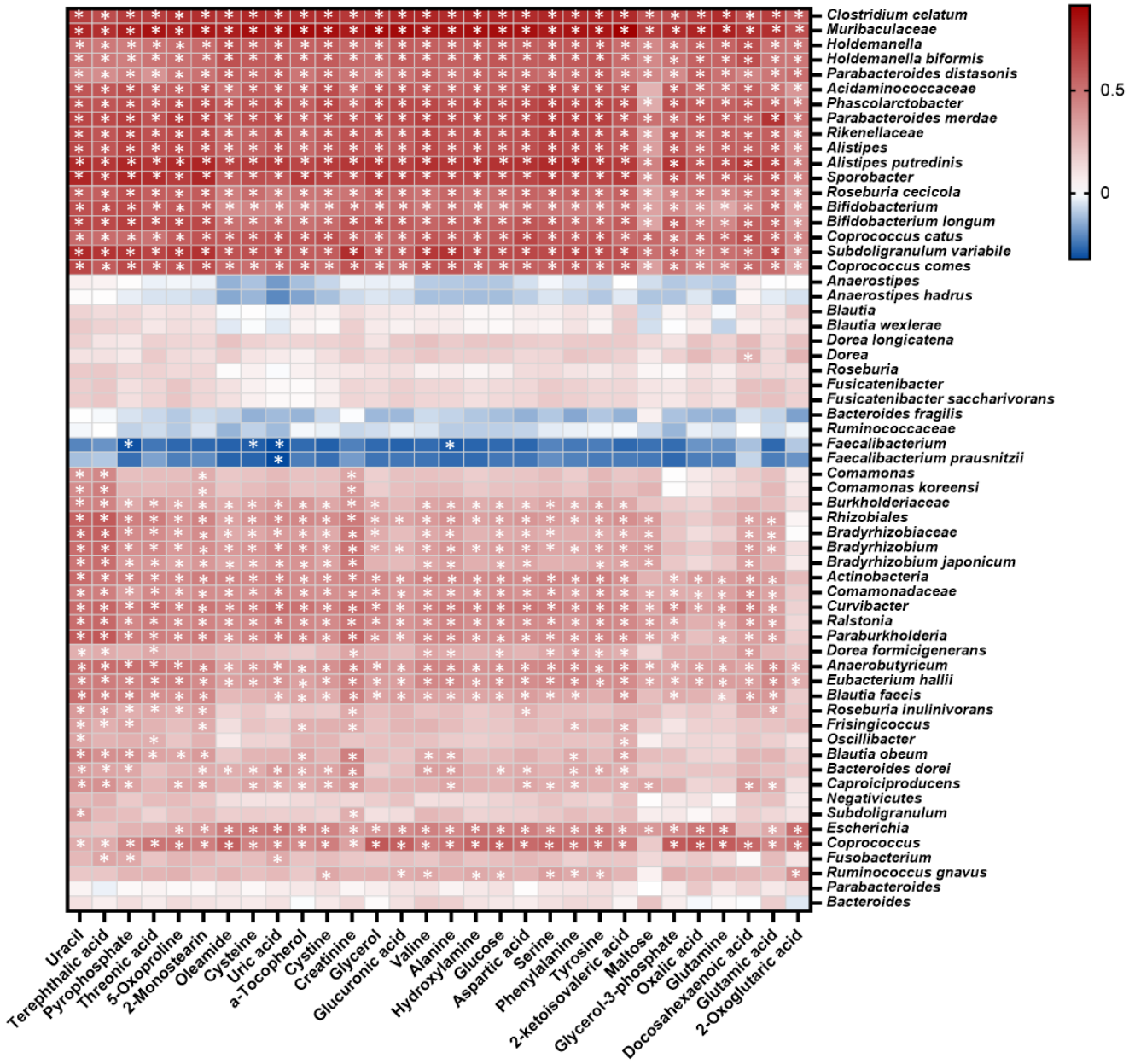

Figure 17. Correlation heatmap of potential microbial and metabolomic biomarkers in UC, CD, and BD. The correlation analysis by Spearman rank correlation between potential microbial and metabolomic biomarkers is shown in the correlation heatmap. Microbial taxa

mainly decreased in UC are mostly positively correlated with most of metabolomic biomarkers, whereas microbial taxa mainly decreased in CD and BD showed negative correlation with most of metabolomic biomarkers. The cells marked with asterisks (*) indicate Spearman correlation analysis with $p < 0.05$. UC: ulcerative colitis, CD: Crohn's disease, BD: Behçet's disease

IV. DISCUSSION

In this integrative analysis of microbiome and metabolome in IBD and intestinal BD, we identified both common and disease-specific profiles of UC, CD, and intestinal BD. The microbial diversity of colon tissue was only reduced in CD, with intestinal BD showing no significant decrease. The microbial taxonomic profile of intestinal BD displayed a pattern more similar to healthy control than UC or CD, and it exhibited distinctive features setting it apart from both UC and CD. However, there were common changes across all three conditions (UC, CD, and intestinal BD), including a decrease in beneficial bacteria responsible for producing short-chain fatty acids such as *Fusicatenibacter saccharivorans*, *Coprococcus comes, Blautia obeum, Dorea formicigenerans,* and *Roseburai ceciola*. Additionally, reductions in genera like *Subdoligranulum* and *Roseburia*, previously mentioned in fecal sample studies of systemic BD patients, were also observed in the intestinal BD of this study. However, these changes were shared characteristics with UC and CD. As a specific alteration unique to intestinal BD, a decrease in the genus *Bacteroides*, particularly the species *Bacteroides fragilis*, was identified. The metabolomic profile of intestinal BD was most similar to CD and distinct from both controls and UC. However, UC, CD, and intestinal BD each exhibited distinct metabolomic profiles. Overall, UC displayed the most dynamic taxonomic changes in the microbiome but exhibited the least

microbial functional alterations and metabolomic changes. In contrast, intestinal BD, while not showing as substantial taxonomic changes as UC or CD, exhibited pronounced functional changes and metabolite alterations. This difference is likely because UC is a condition characterized by inflammation that is more localized to the mucosa, resulting in a diverse range of changes in mucosa-associated microbiota as both its cause and consequence. On the other hand, intestinal BD and CD exhibit a more systemic disease pattern, which could be a reason for the greater number of plasma metabolite changes associated with systemic inflammation and host immune response.

Previous studies have evaluated the composition of gut microbiota in IBD patients and confirmed significant differences of gut microbiota from that of healthy individuals.[5-11] Overall, active IBD is associated with an increased abundance of the phylum Proteobacteria, as well as genera such as *Fusobacterium*, *Enterococcus*, and *Streptococcus*, and species including *Escherichia coli* and *Ruminococcus gnavus*. These taxa consistently showed an increased relative abundance that correlated with IBD activity. Conversely, IBD is linked to the loss of beneficial taxa such as *Faecalibacterium prausnitzii*, *Christensenellaceae*, *Roseburia*, *Bifidobacterium longum*, *Coprococcus*, *Blautia*, and other butyrate-producing bacteria.[5,31-33] However, the results were heterogenous, and few studies evaluated the difference of microbiota between UC and CD within IBD.[5,33,34] In our study, the microbial changes observed in UC and CD were consistent with previous research on IBD. When considering intestinal BD alongside IBD, we identified shared protective taxa that exhibited decreased abundance in all of UC, CD, and intestinal BD. Notably, these taxa have frequently been described as decreased in UC and CD in prior studies except for *Fusicatenibacter*, suggesting that the microbial alterations in intestinal BD follow a similar pattern to those in IBD. Among the five commonly decreased species in our study, *Fusicatenibacter saccharivorans* is less frequently described in IBD. It belonged to the Clostridium subcluster XIVa and was initially isolated and cultured from healthy human feces in 2013.[35] *F. saccharivorans* produces short-chain fatty acids such as lactic acid, acetic acid, and succinic acid, and was reported to be decreased in UC and CD.[36-38] *F.*

saccharivorans play an anti-inflammatory role by inducing IL-10 and prevented murine acute colitis.[36]

The research on the gut microbiome in BD is limited, especially regarding intestinal BD. The previous studies on BD primarily focused on the oral mucosa or saliva microbiome of systemic BD patients. Although some studies have investigated fecal microbiota, there have been no studies analyzing the microbiome of colon tissue in intestinal BD. In the first study that confirmed gut dysbiosis in BD through stool samples in 2015,[39] 22 BD patients (with an unconfirmed precise ratio of those diagnosed with intestinal BD, as only described as 32% having gastrointestinal symptoms) exhibited a decrease in the *Roseburia* genus in fecal microbiota analysis, a finding also observed in our study with the decrease of *Roseburia ceciola*. Additionally, a decrease in the *Subdoligranulum* genus was observed, and our study also yielded the same results. Another study also reported an increase in *Bacteroides uniformis* in the fecal microbiome among systemic BD patients without intestinal involvement,[40] whereas our study did not find a significant difference. Among our intestinal BD patients, 30% of tissue sample donors and 36% of blood sample donors had intestinal BD without systemic BD. Although it is possible that the microbiome characteristics between intestinal BD and systemic BD may be similar, we anticipate that there may be more specific changes in mucosa-associated microbiota analyzed through colon biopsy in intestinal BD. The microbiota that specifically decreased in intestinal BD was *Bacteroides fragilis* in our study. Bacteroidetes is one of the dominant phylum in healthy individuals, and it is known to decrease in patients with IBD. Some members of the *Bacteroides* genus have demonstrated anti-inflammatory functions.[41-43] Moreover, many *Bacteroides* species can break down complex polysaccharides, releasing simple carbohydrate products that other bacteria can use. Previous studies show that *Bacteroides* play a crucial role in the ecological networks of the gut microbiota, and their removal can disrupt these networks.[44] Therefore, *Bacteroides* have the potential to act as 'foundation species' that help maintain the gut microbial community. Considering this, the decrease in *Bacteroides* in intestinal BD may be a possible explanation for pronounced functional

changes and metabolite alterations in intestinal BD, even though it doesn't exhibit as substantial microbial taxonomic changes as UC or CD – a subtle yet impactful shit. Also, some members of the *Bacteroides* genus have demonstrated anti-inflammatory functions. *Bacteroides fragilis*, in particular, and its immunomodulatory symbiosis factor, capsular polysaccharide A (PSA),[45] have been extensively studied and shown to be effective in preventing colitis in murine models.[42,46,47] In the pathogenesis of BD, it shares some common features with autoimmune and autoinflammatory diseases as well as spondyloarthropathies.[3] One suspected triggering infectious agent is herpes simplex virus (HSV)-1, which has a high homology with human proteins like heat-shock proteins. Cross-reaction to autoantigens can lead to an autoimmune response in BD patients.[3,48] PSA and *Bacteroides fragilis* have shown potent immunomodulatory activity in protecting against diseases like herpes simplex encephalitis caused by HSV-1 and autoimmune encephalitis triggered by herpes simplex encephalitis. This protection is achieved by PSA binding to and stimulating intestinal toll-like receptor (TLR) 2-positive plasmacytoid dendritic cells and B cells, leading to the secretion of IL-10. This, in turn, induces regulatory T cells that produce both IL-10 and IFN-γ. These regulatory mechanisms collectively suppress pathogenic inflammatory monocytes and neutrophils.[41] Such immunomodulatory and autoimmune response-suppressing mechanisms associated with *Bacteroides fragilis* may represent a causal link between the decreased abundance of *Bacteroides fragilis* and intestinal BD.

Numerous studies have reported substantial alterations in the gut metabolite profiles of patients with IBD.[10,12,13,49] Metabolite profiling could also discriminate between different forms of IBD, such as CD and UC,[50,51] and could further classify patients with CD as having either ileal or colonic inflammation.[52] Previous metabolomic analysis showed a pronounced separation of CD and control, whereas UC was more heterogeneous.[12] In our study, a similar finding was observed with UC exhibiting the least metabolomic changes. Intestinal BD showed similar metabolomic profiles with CD and is distinct from controls. Metabolite can be analyzed in multiple sample types such as blood, urine, stool, and tissue,

and each biosample provides different biochemical information. Because blood metabolite may provide a systemic metabolism result from the crosstalk of microbiota with the host, we performed metabolomic analysis in the plasma sample. Representative metabolite changes identified in previous studies of IBD, using serum and plasma samples, include alterations in branched-chain amino acids, increased levels of 3-hydroxybutyrate, and decreased levels of glutamine, histidine, tryptophan, and lipids.[53,54] The frequently reported changes in bile acid or short-chain fatty acids are mainly reported from stool samples, and not detected in our study. In our study, glutamate was decreased in all of UC, CD, and intestinal BD. Butyrate-producing commensal bacteria ferment pyruvate to produce butyrate, while certain pathogenic bacteria, such as *Fusobacterium*, utilize glutamate as a substrate for butyrate production.[55] Consequently, dysbiosis, which is commonly observed in IBD and intestinal BD, may contribute to the decreased levels of glutamate observed in our study. Additionally, the bacteria that decreased in all three diseases also possess the enzyme glutamate synthase, which converts glutamine to glutamate. A decrease in these bacteria may contribute to decreased glutamate and increase in glutamine. The unique change of metabolite in intestinal BD was increase in glucuronic acid. Enrichment analysis showed increased pentose and glucuronate interconversions in intestinal BD, and glucuronate isomerase catalyzes change between fructuronic acid and glucuronic acid. Since this enzyme is encoded in genes of bacteria that are decreased in abundance in intestinal BD such as *Bacteroides fragilis* and *Caproiciproducens*, changes in balance may contributed the changed level of glucuronic acid. In CD, hydroxylamine and uric acid were increased in our study. Hydroxylamine, a derivative ammonium, is an intermediate in two important microbial processes of the nitrogen cycle. It is formed during nitrification and also during anaerobic ammonium oxidation.[56] It is a well-known mutagen, moderately toxic and harmful to human. The report on hydroxylamine in IBD is scarce, and further data are needed regarding this metabolite. Uric acid is the terminal product of purine nucleoside metabolism by xanthine dehydrogenase. The increase of *Bacteroides* and the decrease of *Faecalibacterium, Clostridium*, and *Ruminococcus* result in excessive uric acid

production in the liver and insufficient uric acid excretion in the kidney and intestine, raising serum uric acid levels.[57] IBD patients had increased uric acid levels than control, and serum uric acid to creatinine ratio is associated with disease activity in CD.[58] Also, phenylalanine was increased in UC in our study. Phenylalanine has been shown to be disturbed in IBD, but there are inconsistencies regarding increase or decrease in fecal or serum samples. Phenylalanine inhibits TNF-α production and has an anti-inflammatory role, and our study showed a decreased level in UC.[53]

Integrating multi-omics data poses several challenges. Identifying a metabolite as originated from the microbiome can be complex, and pinpointing the specific microorganism responsible for producing or modifying a particular metabolite is even more daunting. While the mechanistic links between host diseases, microorganisms, and metabolites are becoming clearer, significant questions about disease-associated metabolites remain unanswered. These questions encompass whether these metabolites originate from bacteria or result from host metabolism, whether they directly affect bacteria or indirectly influence host physiology, or potentially represent a combination of these scenarios. To address these challenges, it is imperative to move beyond merely identifying correlations between various omics data. Additional investigations, such as comparing metabolites with cultured isolates of microbiota or utilizing germ-free or specific pathogen-free mouse models, are essential.

This study possesses several strengths. Firstly, it is the first investigation to examine mucosa-associated microbiome and metabolome changes in intestinal BD, providing a unique perspective. Additionally, it is the first study to analyze intestinal BD alongside IBD, allowing for a comprehensive exploration of both commonalities and differences. While there have been a few studies on microbiome changes in systemic BD, none have specifically targeted intestinal BD, and they have primarily focused on fecal microbiome analysis. Compositionally distinct from luminal microbiota represented by feces,[59] the mucosa-associated microbiota interacts more directly with host epithelial and immune cells through pattern recognition receptors and other signals.[60]

This study has several limitations. Firstly, due to its cross-sectional design, a single sample may not fully capture the temporal changes in the intestinal microbiome. The stability of the microbial community over time, rather than the specific taxa present at a single time point, can be a strong predictor of disease activity.[61] Additionally, many other factors, such as diet, lifestyle, and medication, were not controlled for, and it's possible that these factors could have influenced the bacterial composition or metabolite profile.[7] Since the subjects were not enrolled in a matched manner across groups, the younger age of CD patients compared to other groups may have also influenced microbial composition. It's also important to note that distinguishing species using 16S rRNA sequencing can be challenging. Furthermore, untargeted metabolomics detected a relatively small number of metabolites, and the samples used for metagenomics analysis were different from those used for metabolite analysis, which limited the sample size for the microbiome-metabolite interaction analysis. Another limitation is that the study included patients who were already receiving treatment, and some changes in the microbiota and metabolites may have normalized due to treatment, limiting their utility as diagnostic markers. However, the microbial changes observed in IBD in this study were broadly consistent with those reported in previous studies.

V. CONCLUSION

This study performed an integrated analysis of the gut microbiome on tissue and stool samples by 16S rRNA sequencing and plasma metabolite profiling by GC-MS-TOF and UPLC–Q–TOF–MS analysis in patients with intestinal BD as well as UC and CD compared with healthy control. The microbial taxonomic profile of intestinal BD displayed a pattern more similar to healthy control than UC or CD, and it exhibited distinctive features setting it apart from both UC and CD. The metabolomic profile of intestinal BD was most similar to CD and distinct from both controls and UC. Intestinal BD exhibited pronounced functional changes and metabolite alterations, while not showing as substantial microbial taxonomic changes as UC or CD. We identified potential microbial and metabolomic

biomarkers that can either group the diseases together or distinguish each of UC, CD, and intestinal BD.

REFERENCES

1. Imhann F, Vich Vila A, Bonder MJ, Fu J, Gevers D, Visschedijk MC, et al. Interplay of host genetics and gut microbiota underlying the onset and clinical presentation of inflammatory bowel disease. Gut 2018;67:108-19.
2. Davatchi F, Chams-Davatchi C, Shams H, Shahram F, Nadji A, Akhlaghi M, et al. Behcet's disease: epidemiology, clinical manifestations, and diagnosis. Expert Rev Clin Immunol 2017;13:57-65.
3. Leccese P, Alpsoy E. Behçet's Disease: An Overview of Etiopathogenesis. Front Immunol 2019;10:1067.
4. Fraher MH, O'Toole PW, Quigley EM. Techniques used to characterize the gut microbiota: a guide for the clinician. Nat Rev Gastroenterol Hepatol 2012;9:312-22.
5. Pittayanon R, Lau JT, Leontiadis GI, Tse F, Yuan Y, Surette M, et al. Differences in Gut Microbiota in Patients With vs Without Inflammatory Bowel Diseases: A Systematic Review. Gastroenterology 2020;158:930-46.e1.
6. Dovrolis N, Drygiannakis I, Filidou E, Kandilogiannakis L, Arvanitidis K, Tentes I, et al. Gut Microbial Signatures Underline Complicated Crohn's Disease but Vary Between Cohorts; An In Silico Approach. Inflamm Bowel Dis 2019;25:217-25.
7. Gilbert JA, Blaser MJ, Caporaso JG, Jansson JK, Lynch SV, Knight R. Current understanding of the human microbiome. Nat Med 2018;24:392-400.
8. Pascal V, Pozuelo M, Borruel N, Casellas F, Campos D, Santiago A, et al. A microbial signature for Crohn's disease. Gut 2017;66:813-22.
9. Gevers D, Kugathasan S, Denson LA, Vázquez-Baeza Y, Van Treuren W, Ren B, et al. The treatment-naive microbiome in new-onset Crohn's disease. Cell Host Microbe 2014;15:382-92.

10. Metwaly A, Dunkel A, Waldschmitt N, Raj ACD, Lagkouvardos I, Corraliza AM, et al. Integrated microbiota and metabolite profiles link Crohn's disease to sulfur metabolism. Nat Commun 2020;11:4322.
11. Vester-Andersen MK, Mirsepasi-Lauridsen HC, Prosberg MV, Mortensen CO, Träger C, Skovsen K, et al. Increased abundance of proteobacteria in aggressive Crohn's disease seven years after diagnosis. Sci Rep 2019;9:13473.
12. Franzosa EA, Sirota-Madi A, Avila-Pacheco J, Fornelos N, Haiser HJ, Reinker S, et al. Gut microbiome structure and metabolic activity in inflammatory bowel disease. Nat Microbiol 2019;4:293-305.
13. Kolho KL, Pessia A, Jaakkola T, de Vos WM, Velagapudi V. Faecal and Serum Metabolomics in Paediatric Inflammatory Bowel Disease. J Crohns Colitis 2017;11:321-34.
14. Scoville EA, Allaman MM, Brown CT, Motley AK, Horst SN, Williams CS, et al. Alterations in Lipid, Amino Acid, and Energy Metabolism Distinguish Crohn's Disease from Ulcerative Colitis and Control Subjects by Serum Metabolomic Profiling. Metabolomics 2018;14:17.
15. Wilmanski T, Rappaport N, Earls JC, Magis AT, Manor O, Lovejoy J, et al. Blood metabolome predicts gut microbiome alpha-diversity in humans. Nat Biotechnol 2019;37:1217-28.
16. Gomollon F, Dignass A, Annese V, Tilg H, Van Assche G, Lindsay JO, et al. 3rd European Evidence-based Consensus on the Diagnosis and Management of Crohn's Disease 2016: Part 1: Diagnosis and Medical Management. J Crohns Colitis 2017;11:3-25.
17. Magro F, Gionchetti P, Eliakim R, Ardizzone S, Armuzzi A, Barreiro-de Acosta M, et al. Third European Evidence-based Consensus on Diagnosis and Management of Ulcerative Colitis. Part 1: Definitions, Diagnosis, Extra-intestinal Manifestations, Pregnancy, Cancer Surveillance, Surgery, and Ileo-anal Pouch Disorders. J Crohns Colitis 2017;11:649-70.

18. Cheon JH, Kim ES, Shin SJ, Kim TI, Lee KM, Kim SW, et al. Development and validation of novel diagnostic criteria for intestinal Behcet's disease in Korean patients with ileocolonic ulcers. Am J Gastroenterol 2009;104:2492-9.
19. Cheon JH, Han DS, Park JY, Ye BD, Jung SA, Park YS, et al. Development, validation, and responsiveness of a novel disease activity index for intestinal Behcet's disease. Inflamm Bowel Dis 2011;17:605-13.
20. Kim BS, Kim JN, Yoon SH, Chun J, Cerniglia CE. Impact of enrofloxacin on the human intestinal microbiota revealed by comparative molecular analysis. Anaerobe 2012;18:310-20.
21. Kim BS, Song MY, Kim H. The anti-obesity effect of Ephedra sinica through modulation of gut microbiota in obese Korean women. J Ethnopharmacol 2014;152:532-9.
22. Yun KH, Lee HS, Nam OH, Moon CY, Lee JH, Choi SC. Analysis of bacterial community profiles of endodontically infected primary teeth using pyrosequencing. Int J Paediatr Dent 2017;27:56-65.
23. Jeon YS, Lee K, Park SC, Kim BS, Cho YJ, Ha SM, et al. EzEditor: a versatile sequence alignment editor for both rRNA- and protein-coding genes. Int J Syst Evol Microbiol 2014;64:689-91.
24. Yoon SH, Ha SM, Kwon S, Lim J, Kim Y, Seo H, et al. Introducing EzBioCloud: a taxonomically united database of 16S rRNA gene sequences and whole-genome assemblies. Int J Syst Evol Microbiol 2017;67:1613-7.
25. Langille MG, Zaneveld J, Caporaso JG, McDonald D, Knights D, Reyes JA, et al. Predictive functional profiling of microbial communities using 16S rRNA marker gene sequences. Nat Biotechnol 2013;31:814-21.
26. Pavoine S, Dufour AB, Chessel D. From dissimilarities among species to dissimilarities among communities: a double principal coordinate analysis. J Theor Biol 2004;228:523-37.
27. Ramette A. Multivariate analyses in microbial ecology. FEMS Microbiol Ecol

2007;62:142-60.

28. Kelly BJ, Gross R, Bittinger K, Sherrill-Mix S, Lewis JD, Collman RG, et al. Power and sample-size estimation for microbiome studies using pairwise distances and PERMANOVA. Bioinformatics 2015;31:2461-8.
29. Goeman JJ, van de Geer SA, de Kort F, van Houwelingen HC. A global test for groups of genes: testing association with a clinical outcome. Bioinformatics 2004;20:93-9.
30. Glickman ME, Rao SR, Schultz MR. False discovery rate control is a recommended alternative to Bonferroni-type adjustments in health studies. J Clin Epidemiol 2014;67:850-7.
31. Metwaly A, Reitmeier S, Haller D. Microbiome risk profiles as biomarkers for inflammatory and metabolic disorders. Nat Rev Gastroenterol Hepatol 2022;19:383-97.
32. Qiu P, Ishimoto T, Fu L, Zhang J, Zhang Z, Liu Y. The Gut Microbiota in Inflammatory Bowel Disease. Front Cell Infect Microbiol 2022;12:733992.
33. Schirmer M, Garner A, Vlamakis H, Xavier RJ. Microbial genes and pathways in inflammatory bowel disease. Nat Rev Microbiol 2019;17:497-511.
34. Vich Vila A, Imhann F, Collij V, Jankipersadsing SA, Gurry T, Mujagic Z, et al. Gut microbiota composition and functional changes in inflammatory bowel disease and irritable bowel syndrome. Sci Transl Med 2018;10.
35. Takada T, Kurakawa T, Tsuji H, Nomoto K. Fusicatenibacter saccharivorans gen. nov., sp. nov., isolated from human faeces. Int J Syst Evol Microbiol 2013;63:3691-6.
36. Takeshita K, Mizuno S, Mikami Y, Sujino T, Saigusa K, Matsuoka K, et al. A Single Species of Clostridium Subcluster XIVa Decreased in Ulcerative Colitis Patients. Inflamm Bowel Dis 2016;22:2802-10.
37. Gryaznova MV, Solodskikh SA, Panevina AV, Syromyatnikov MY, Dvoretskaya YD, Sviridova TN, et al. Study of microbiome changes in patients with ulcerative

colitis in the Central European part of Russia. Heliyon 2021;7:e06432.

38. Ma X, Lu X, Zhang W, Yang L, Wang D, Xu J, et al. Gut microbiota in the early stage of Crohn's disease has unique characteristics. Gut Pathog 2022;14:46.
39. Consolandi C, Turroni S, Emmi G, Severgnini M, Fiori J, Peano C, et al. Behcet's syndrome patients exhibit specific microbiome signature. Autoimmun Rev 2015;14:269-76.
40. Kim JC, Park MJ, Park S, Lee ES. Alteration of the Fecal but Not Salivary Microbiome in Patients with Behçet's Disease According to Disease Activity Shift. Microorganisms 2021;9.
41. Ramakrishna C, Kujawski M, Chu H, Li L, Mazmanian SK, Cantin EM. Bacteroides fragilis polysaccharide A induces IL-10 secreting B and T cells that prevent viral encephalitis. Nat Commun 2019;10:2153.
42. Zhang W, Zhou Q, Liu H, Xu J, Huang R, Shen B, et al. Bacteroides fragilis strain ZY-312 facilitates colonic mucosa regeneration in colitis via motivating STAT3 signaling pathway induced by IL-22 from ILC3 secretion. Front Immunol 2023;14:1156762.
43. Porter NT, Luis AS, Martens EC. Bacteroides thetaiotaomicron. Trends Microbiol 2018;26:966-7.
44. Trosvik P, de Muinck EJ. Ecology of bacteria in the human gastrointestinal tract--identification of keystone and foundation taxa. Microbiome 2015;3:44.
45. Mazmanian SK, Liu CH, Tzianabos AO, Kasper DL. An immunomodulatory molecule of symbiotic bacteria directs maturation of the host immune system. Cell 2005;122:107-18.
46. Chang YC, Ching YH, Chiu CC, Liu JY, Hung SW, Huang WC, et al. TLR2 and interleukin-10 are involved in Bacteroides fragilis-mediated prevention of DSS-induced colitis in gnotobiotic mice. PLoS One 2017;12:e0180025.
47. Mazmanian SK, Round JL, Kasper DL. A microbial symbiosis factor prevents intestinal inflammatory disease. Nature 2008;453:620-5.

48. Studd M, McCance DJ, Lehner T. Detection of HSV-1 DNA in patients with Behçet's syndrome and in patients with recurrent oral ulcers by the polymerase chain reaction. J Med Microbiol 1991;34:39-43.
49. Lloyd-Price J, Arze C, Ananthakrishnan AN, Schirmer M, Avila-Pacheco J, Poon TW, et al. Multi-omics of the gut microbial ecosystem in inflammatory bowel diseases. Nature 2019;569:655-62.
50. Marchesi JR, Holmes E, Khan F, Kochhar S, Scanlan P, Shanahan F, et al. Rapid and noninvasive metabonomic characterization of inflammatory bowel disease. J Proteome Res 2007;6:546-51.
51. Le Gall G, Noor SO, Ridgway K, Scovell L, Jamieson C, Johnson IT, et al. Metabolomics of fecal extracts detects altered metabolic activity of gut microbiota in ulcerative colitis and irritable bowel syndrome. J Proteome Res 2011;10:4208-18.
52. Jansson J, Willing B, Lucio M, Fekete A, Dicksved J, Halfvarson J, et al. Metabolomics reveals metabolic biomarkers of Crohn's disease. PLoS One 2009;4:e6386.
53. Bauset C, Gisbert-Ferrándiz L, Cosín-Roger J. Metabolomics as a Promising Resource Identifying Potential Biomarkers for Inflammatory Bowel Disease. J Clin Med 2021;10.
54. Gallagher K, Catesson A, Griffin JL, Holmes E, Williams HRT. Metabolomic Analysis in Inflammatory Bowel Disease: A Systematic Review. J Crohns Colitis 2021;15:813-26.
55. Anand S, Kaur H, Mande SS. Comparative In silico Analysis of Butyrate Production Pathways in Gut Commensals and Pathogens. Front Microbiol 2016;7:1945.
56. Arp DJ, Stein LY. Metabolism of inorganic N compounds by ammonia-oxidizing bacteria. Crit Rev Biochem Mol Biol 2003;38:471-95.
57. Tong S, Zhang P, Cheng Q, Chen M, Chen X, Wang Z, et al. The role of gut

microbiota in gout: Is gut microbiota a potential target for gout treatment. Front Cell Infect Microbiol 2022;12:1051682.

58. Zhu F, Feng D, Zhang T, Gu L, Zhu W, Guo Z, et al. Altered uric acid metabolism in isolated colonic Crohn's disease but not ulcerative colitis. J Gastroenterol Hepatol 2019;34:154-61.

59. Parthasarathy G, Chen J, Chen X, Chia N, O'Connor HM, Wolf PG, et al. Relationship Between Microbiota of the Colonic Mucosa vs Feces and Symptoms, Colonic Transit, and Methane Production in Female Patients With Chronic Constipation. Gastroenterology 2016;150:367-79.e1.

60. Fukata M, Arditi M. The role of pattern recognition receptors in intestinal inflammation. Mucosal Immunol 2013;6:451-63.

61. Halfvarson J, Brislawn CJ, Lamendella R, Vázquez-Baeza Y, Walters WA, Bramer LM, et al. Dynamics of the human gut microbiome in inflammatory bowel disease. Nat Microbiol 2017;2:17004.

ABSTRACT(IN KOREAN)

마이크로바이옴과 대사체의 통합 분석을 통한 염증성 장질환과 베체트 장염의 질병 특이적 특징 규명

<지도교수 천재희>

연세대학교 대학원 의학과

박예현

배경 및 목적: 장내 마이크로바이옴과 대사체 변화는 염증성 장질환인 궤양성 대장염과 크론병과 연관된 것으로 알려져 있다. 그러나 염증성 장질환과 임상적으로 공통점이 많은 베체트 장염에서는 이러한 마이크로바이옴이나 대사체 변화에 대한 연구가 부족하며, 병인론적으로 베체트 장염과 염증성 장질환의 유사성이 제기되고 있으나 아직 베체트 장염의 병인에 대해서는 많은 연구가 필요하다. 본 연구는 베체트 장염 환자의 장 내 마이크로바이옴 특징 및 기능적 변화, 대사체의 변화를 염증성 장질환 및 대조군과 비교하여 확인하고, 베체트 장염과 궤양성 대장염, 크론병을 구분하는 데 도움이 되는 미생물 및 대사체 마커를 발견하기 위해 시행되었다.

연구 방법: 진단 대장내시경 검사를 받는 성인 염증성 장질환 및 베체트 장염 환자와 건강한 자원자를 대상으로 회맹부에서 획득한 대장 조직 샘플을 이용하여 16S 리보솜 RNA (rRNA) 서열 분석을 시행하였으며, 미생물 군집의 다양성, 분류학적 조성 및 기능적 특징을 대조군, 궤양성 대장염, 크론병 및 베체트 장염 그룹간 비교하였다. 또 대조군과 염증성 장질환 환자의 대변 샘플을 16S rRNA 서열 분석을 위해 수집하고 분석하였다. 대조군, 궤양성 대장염, 크론병 및 베체트 장염 환자로부터 혈액을 채취하고 가스 및 액체 크로마토그래피 질량분석을 이용하여 혈장 대사체 분석을 시행하였다.

결과: 총 100명의 환자 (35명의 궤양성 대장염, 30명의 크론병, 35명의 베체트 장염) 및 41명의 건강한 자원자가 연구에 참여하였다. 73개의 조직 샘플 (12명의 대조군, 24명 궤양성 대장염, 14명 크론병, 23명 베체트장염)과 19개의

대변 샘플 (5명 대조군, 9명 궤양성 대장염, 5명 크론병)에 대한 16S rRNA 서열 분석을 시행하였고, 100개의 혈액 샘플 (25명 대조군, 24명 궤양성 대장염, 26명 크론병, 25명 베체트 장염)에 대한 대사체 분석을 시행하였다. 대장 조직의 미생물 다양성은 크론병에서만 의미 있게 감소하였으며, 베체트 장염에서는 유의한 감소를 보이지 않았다. 베체트 장염의 미생물 분류상 특징은 궤양성 대장염이나 크론병보다 대조군과 더 유사한 양상을 나타내며, 염증성 장질환과는 뚜렷이 구분되는 특징을 보였다. 그러나 염증성 장질환과 베체트 장염에서 공통적인 변화도 확인되었으며, 단쇄지방산을 생성하는 유익균 중 다섯 가지 (*Fusicatenibacter saccharivorans*, *Coprococcus comes*, *Blautia obeum*, *Dorea formicigenerans*, and *Roseburai ceciola*)의 감소였다. 베체트 장염에서는 추가적으로 *Subdoligranulum variable*과 *Blautia wexlerae*의 감소가 확인되었는데 이는 궤양성 대장염 또는 크론병과 공통된 특징이었다. 베체트 장염에 특이적인 변화로 *Bacteroides* 속, 특히 *Bacteroides fragilis* 종의 감소가 확인되었다. 베체트 장염의 대사체 특징은 크론병과 가장 유사하였고, 대조군이나 궤양성 대장염과는 구분되었다. 그러나 궤양성 대장염, 크론병, 베체트 장염 각각 특징적인 대사체 결과를 나타냈다. 전반적으로 베체트 장염은 궤양성 대장염이나 크론병처럼 큰 미생물 변화를 나타내지 않으면서도, 에너지 대사, 아미노산, 탄수화물 및 지질 대사, 보조 인자 및 비타민 대사, 뉴클레오타이드 대사, 유전 정보 처리 등의 대사 경로가 증가되어 있고 그에 해당하는 대사체 변화를 보였으며, 이러한 변화가 미생물 변화와 잘 연관지어 나타남을 확인할 수 있었다.

결론: 염증성 장질환과 베체트 장염에서의 미생물 및 대사체 통합 분석에서 베체트 장염은 대조군 및 염증성 장질환과 공유되는 특징과 함께 구분되는 질환 특이적 특징을 나타내어, 이 질환들간의 유사성 및 차이점을 유추해 볼 수 있었고 이러한 미생물 및 대사체 특징은 추후 이들 질환의 진단 및 감별 진단의 마커로서 사용될 가능성이 있다.

핵심되는 말: 베체트 장염, 크론병, 궤양성 대장염, 마이크로바이옴, 대사체